Journal of Hydrology 645 (2024) 132230

Contents lists available at ScienceDirect

Journal of Hydrology

journal homepage: www.elsevier.com/locate/jhydrol

Research papers

Integration of multiple observations for validation of mechanisms of earthquake-triggered groundwater level Anomalies: 2016 Taiwan Meinong earthquake

Shih-Jung Wang [a,b,*], Yan-Yao Lin [a], Ying-Han Chen [a], Chia-Lin Chung [c], Wen-Chi Lai [d], Chien-Chung Ke [e]

[a] *Graduate Institute of Applied Geology, National Central University, 300 Zhongda Rd., Zhongli District, Taoyuan City 32001, Taiwan*
[b] *Department of Earth Sciences, National Central University, 300 Zhongda Rd., Zhongli District, Taoyuan City 32001, Taiwan*
[c] *Earthquake Disaster & Risk Evaluation and Management Center (E-DREaM), National Central University, Taoyuan City 32001, Taiwan*
[d] *Disaster Prevention Research Center, National Cheng Kung University, 1 University Road, Tainan City 70101, Taiwan*
[e] *Advanced Geological Research Task Force, Sinotech Engineering Consultants, Inc., Taipei City 114065, Taiwan*

ARTICLE INFO

Keywords:
Multi-depth groundwater level variation
Strong ground motion
Hydrogeological property
Soil liquefaction
Triggering mechanism
Taiwan Meinong earthquake

ABSTRACT

This study analyzes multi-depth groundwater level data and integrated observation data to validate the previously proposed mechanisms of hydrological anomalies triggered by the 2016 M6.4 Meinong earthquake in Taiwan. The main influence area was northwest of the epicenter, which may be due to the blind fault rupture, intensity distribution, and hydrogeological properties. The step changes in groundwater level do not fit the concept of epicentral distance, static stress–strain theory, or the focal mechanism. The distribution of step changes in groundwater level have a pattern similar to that of horizontal peak ground velocity. The results imply that these changes may be driven by dynamic stress–strain, instead of static stress–strain. The minimum horizontal peak ground velocity and acceleration of the Meinong earthquake, which induced obvious step changes in groundwater level and soil liquefaction, are provided. The pressure dissipation ability of an aquifer (e.g., transmissivity) may affect the persistence of groundwater responses. Four wells located near the surface rupture area, which has cemented or partial cemented geological material, showed an obvious step decrease in the groundwater level at a deep depth and all wells showed an increase in the groundwater level at a shallow depth. These decreases and increases of the groundwater level at different depths have different mechanisms, which are discussed in this study. The integrated observations made during the Meinong earthquake show that ground motion and the hydraulic properties might be important factors in hydrological anomalies. The results of this study are an important reference for further studies on earthquake hydrology.

1. Introduction

Earthquakes can induce hydrological anomalies, such as groundwater level, chemical composition, and temperature variations, river discharge increases, soil liquefaction, and mud volcano eruption (Wang and Manga, 2010, 2021). Earthquake-induced groundwater level variations have been observed all over the world (e.g., He and Singh, 2019; Lutzky et al., 2020; Roeloffs, 1998, Wang et al., 2015c) and river discharge increases have been widely reported (e.g., Koizumi et al., 2019; Manga and Rowland, 2009; Manga et al., 2003; Montgomery and Manga, 2003; Rojstaczer et al., 1995). Groundwater level variations triggered by earthquakes can be approximately separated into oscillation changes and step changes. The former are mainly induced by dynamic seismic waves and the latter are mainly induced by volumetric strain or aquifer property changes (e.g., Wang and Manga, 2010, 2021), though some unusual phenomena have also been reported (Wang and Manga, 2010, 2021). Oscillation data from a device with a 1-Hz sampling interval might contain a hydroseismogram signal in the intermediate and far fields (Brodsky et al., 2003; Cooper et al., 1965; He et al., 2017, 2020; Kitagawa et al., 2011). In contrast, for small-sampling-interval records, the maximum oscillation value depends on the sampling interval and thus such records might not provide information on

* Corresponding author at: Graduate Institute of Applied Geology, National Central University, 300 Zhongda Rd., Zhongli District, Taoyuan City 32001, Taiwan.
E-mail address: sjwang@ncu.edu.tw (S.-J. Wang).

https://doi.org/10.1016/j.jhydrol.2024.132230
Received 14 December 2023; Received in revised form 1 September 2024; Accepted 8 October 2024
Available online 19 October 2024

the physical behavior of an aquifer. Step changes are thus commonly used to investigate the mechanism of earthquake-induced groundwater level variations (Wang et al., 2015c). In addition to oscillation changes and step changes, gradual changes, sustained changes, and their combination have been observed (e.g., Cox et al., 2012; Wang and Manga, 2010, 2021), indicating that the mechanism of groundwater level variations is complex.

Several mechanisms have been proposed for step changes in groundwater level, including stress–strain variations (e.g., Akita and Matsumoto, 2004; Chia et al., 2008; Ge and Stover, 2000; Roeloffs, 1996; Wakita, 1975;; Wang et al., 2015c, 2017), undrained consolidation (e.g., Holzer and Youd, 2007; Wang and Chia, 2008; Wang et al., 2001), and permeability enhancement (Brodsky et al., 2003; Elkhoury et al., 2006; Kinoshita et al., 2015; Manga et al., 2012; Matsumoto et al., 2003; Rutter et al., 2016; Wang and Chia, 2008; Xue et al., 2013). Groundwater level variations triggered by an earthquake can be estimated using a dislocation model for a rock system (e.g., Jonsson et al., 2003), but may not for an alluvial fan area (e.g., Koizumi et al., 2004). Undrained consolidation is used for uncemented porous media. This mechanism describes decreases in porosity and permeability in porous media and an increase in pore water pressure, which is mainly due to the effect of dynamic waves. Soil liquefaction is a special case where the pore water pressure is equal to (or larger than) the total stress and the effective stress reaches zero, making porous media liquefy (Terzaghi, 1925). Permeability enhancement commonly occurs in cemented or partially cemented porous media or rock systems, which implies that earthquakes damage the original media (Shalev et al., 2016b, 2021). The driving force could be both the static stress or dynamic stress if the energy is large enough (Wang and Manga, 2021). In this mechanism, an earthquake can create new paths for groundwater to flow or pore water pressure to propagate (Wang et al., 2016). The groundwater level can increase or decrease depending on the original situation (Shi et al., 2015). Different mechanisms may induce step changes in groundwater level; therefore various types of observation are needed to identify a given mechanism.

The Meinong earthquake occurred in southwestern Taiwan in 2016. It had a local magnitude of 6.6, a moment magnitude of 6.4, and a hypocentral depth of 14.6 km. The largest seismic intensity, which induced the largest damage, was in an area relatively far away from the epicenter. The seismic intensity was small in the area close to the epicenter. The distribution of seismic intensity had significant azimuths and the intensity did not decrease with increasing epicentral distance (Wu et al., 2017). This earthquake might thus have induced unusual hydrological responses, providing a good opportunity to validate the mechanism of hydrological variations triggered by earthquakes. Previous studies on the hydrological responses triggered by the Meinong earthquake include those on a suspected radon gas precursor (Fu et al., 2017; Kuo et al., 2018), a mud volcano eruption (Huang et al., 2016), soil liquefaction (Lu et al., 2017), deep fluid pressure propagation (Hsu et al., 2020; Huang et al., 2016), and groundwater level variations (Feng et al., 2016; Lai et al., 2016; Liu, 2018). The radon gas investigations focused on the precursor and the monitoring stations located outside the plain area. The studies on the mud volcano eruption and soil liquefaction did not thoroughly discuss the associated physical mechanism. Previous studies on groundwater level anomalies presented only preliminary results; no other observations were included. Therefore, the mechanisms of the hydrological anomalies triggered by the Meinong earthquake have not been fully investigated. The present study thus collected more data and conducted a complete analysis to determine the associated mechanisms.

The Taiwan Water Resources Agency (WRA) has developed a high-density network of groundwater monitoring wells in the ten groundwater regions in Taiwan. The wells are installed at multiple depths, and thus have a three-dimensional distribution, making their observations of groundwater levels important for studying earthquake-induced groundwater anomalies (Wang and Manga, 2010). The WRA has also installed river gauges and constructed rainfall stations, which provide surface water and climate data for the assessment of hydrological conditions. Furthermore, the Taiwan Geological Survey and Mining Management Agency (GSMMA) has constructed dozens of groundwater wells in mountainous regions and the Taiwan Central Weather Administration (CWA) has constructed six high-sampling-rate (1 Hz) groundwater observation stations in Taiwan, which provide additional information for mechanism validation. The first goal of this study is the collection of various data and the identification of the spatial hydrological anomalies triggered by the Meinong earthquake to examine the unique phenomena of the hydrological response. Different observations and phenomena triggered by earthquakes could be correlated and thus could be used to validate mechanisms. For example, the distribution of earthquake intensity can be affected by fault rupture propagation and hydrogeological properties (site effect), surface displacement can be caused by fault movement and soil liquefaction (related to hydrogeology, pore water pressure, and ground motion), and hydrological anomalies can be caused by groundwater and surface water exchange (can be affected by surface rupture, media damage, or ground motion). The second goal of this study is the use of integrated observation data and analysis results to validate previously proposed mechanisms and determine the limitations of these mechanisms.

In this study, various groundwater level and river discharge observations during the Meinong earthquake are analyzed. Some anomalous phenomena are illustrated. The driving factors for the step changes in groundwater level are discussed based on static and dynamic stress–-strain concepts. The collected seismic data and hydrogeological properties are compared with the responses of the groundwater level. The mechanisms that caused opposite responses at multi-layer groundwater level observation wells are discussed. This study provides high-density groundwater level observations at various depths (from plains to mountains) and for various sampling intervals. These observations are used to validate previously proposed mechanisms and determine the limitations of these mechanisms. Some new concepts are proposed to provide an important reference for further studies on earthquake hydrology.

2. Study Background

2.1. Meinong earthquake

The Meinong earthquake occurred in Meinong District, Kaohsiung City, in southwestern Taiwan, at 3:57 (local time, apply to all the time used in this study) on February 6, 2016. It had a local magnitude of 6.6, a moment magnitude of 6.4, and a hypocentral depth of 14.6 km (as announced by the CWA, on their website: https://scweb.cwa.gov.tw/en-us/earthquake/details/EE2016020603572666006). The focal mechanism indicates a reverse fault with a strike-slip component (Fig. 1). However, the exact fault has not been identified because this earthquake occurred along a blind fault. The largest intensity, namely 7 on the modified Mercalli intensity scale, was in Hsinhua District, Tainan. Although the Meinong earthquake occurred in Kaohsiung City, the largest damage was in Tainan City, which is inconsistent with the decay of energy with distance from the epicenter. Researchers have conducted observations and analyses to determine the cause of this inconsistency. Lin et al. (2018) reported that this earthquake event was an earthquake sequence. The first earthquake (foreshock), denoted as EQ1, occurred in Meinong District; it had a moment magnitude of 5.5 and a hypocentral depth of 14.6 km. The second earthquake (main shock), denoted as EQ2, occurred 5.3 s later in Neimen District (near Tainan City); it had a moment magnitude of 6.18 and a hypocentral depth of 15 km. The epicenters and their focal mechanisms are shown in Fig. 1. The second earthquake was defined as the main shock by Lin et al. (2018) because the largest intensity and damage were mainly in Tainan City, not in Kaohsiung City. The first and second earthquakes were located in areas close to Pingtung and Chianan plains, respectively. To understand the

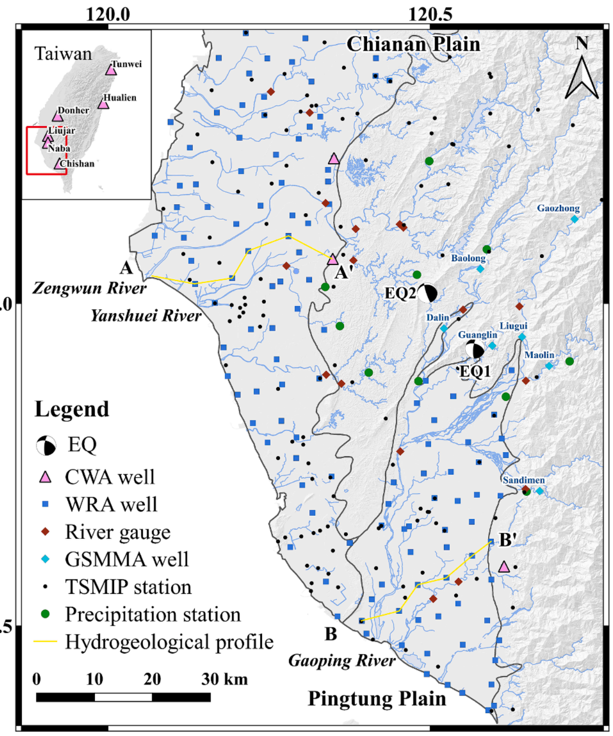

Fig. 1. Study area and distribution of observation stations and epicenters. EQ1 and EQ2 are the epicenters of the first and second earthquakes, respectively, in the earthquake sequence. The first earthquake occurred in Meinong District with a moment magnitude of 5.5 and the second earthquake occurred in Neimen District with a moment magnitude of 6.18 (Lin et al., 2018). The Central Weather Administration announced that the Meinong earthquake was located at the first epicenter with a moment magnitude of 6.4. Black lines delineate the plain areas. Yellow lines are the traces for the two hydrogeological profiles in Chianan and Pingtung plains, respectively (see Fig. 2). (For interpretation of the references to color in this figure legend, the reader is referred to the web version of this article.)

groundwater hydrological responses in these two areas to the Meinong earthquake, data from Chianan and Pingtung plains (see Fig. 1) were collected for comparison.

2.2. Hydrogeological setting

Chianan Plain (area: ~2,500 km^2) is located in western Taiwan between the Taiwan Strait to the west and the Western Foothill Belt of the Central Range to the east (Fig. 1). The depositional environment of Chianan Plain is the Holocene-Pleistocene continental shelf of a littoral sea and is mostly composed of silt and clay (Lu et al., 2008). Pingtung Plain (area: ~1,200 km^2) is located in southwestern Taiwan. It is bounded by the Taiwan Strait to the south and Chishan Fault and Chaochou Fault to the west and east, respectively (Fig. 1). The sediment of Pingtung Plain is mainly deposited by transgression-regression cycles in the Quaternary. The materials are the Linkou conglomerate, an older alluvium, and a recent alluvium with three subunits, namely coarse gravel, alternating gravel and sand, and fine sediments (Ting et al., 1998; Tran et al., 2024). More information on the hydrogeological environments in Chianan and Pingtung plains can be found in the studies of Sengupta et al. (2014) and Ting et al. (1998), respectively. The hydrogeological environments are different in Chianan and Pingtung plains and thus their hydrogeological compositions are different, which might induce a difference in groundwater level responses triggered by earthquakes.

Two selected hydrogeological profiles, constructed by the GSMMA, for Chianan and Pingtung plains are shown in Fig. 2. Fig. 2a shows the hydrogeological profile for Chianan Plain. In the conceptual layer system, four aquifers and three aquitards are defined within a depth of 250 m. The horizontal continuity of the aquifer is relatively short because the main material in this area is fine grain particles (clay and fine sand), leading to a largely confined aquifer system. In a well-confined aquifer, the pore water pressure variations triggered by earthquakes can persist for a relatively long time. A soft material is sensitive to seismic site effects (Seed and Idriss, 1982), which can induce relatively large variations in groundwater level. Two CWA wells (Naba and Liujar wells) in Chianan Plain with a sampling interval of 1 Hz were selected due to their high sensitivity to groundwater level variations triggered by earthquakes (Lai et al., 2010). Fig. 2b shows the hydrogeological profile for Pingtung Plain. In the conceptual layer system, four aquifers and three aquitards are defined within around 250 m. The aquifer layers are thicker compared with those in Chianan Plain. The distribution of aquitards is scattered and does not fully cover the area of Pingtung Plain, making the aquifer poorly confined, and thus the groundwater level variations triggered by earthquakes quickly dissipate. There is a CWA well (Chishan well) located in Pingtung Plain.

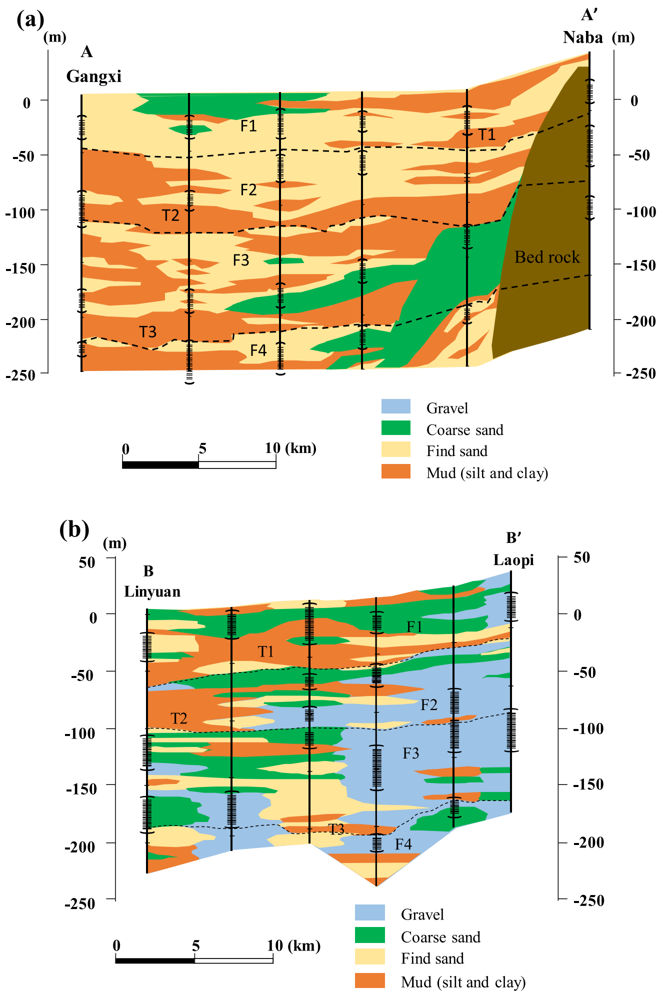

Fig. 2. Selected hydrogeological profiles for (a) Chianan and (b) Pingtung plains. The traces of the profile are shown in Fig. 1. “F” and “T” indicate an aquifer and an aquitard, respectively, and the subsequent numbers indicate the sequence of the aquifer or aquitard. The horizontal dashed lines show the conceptual separation of the layers. The vertical dark lines indicate the wells and the short lines enclosed in brackets indicate the opened screen in that well (modified from the hydrogeological profiles at http://hydrogis.moeacgs.gov.tw [in Chinese] created by the Taiwan Geology Survey and Mining Management Agency).

2.3. Seismograph network

Taiwan, which is located in the Pacific Ring of Fire, is hit by around 24,000 earthquakes annually (based on observations of earthquakes with a local magnitude larger than 0 conducted by the CWA in the period 1991–2020). Therefore, the CWA and some research institutes have installed various kinds of seismograph at a high density in Taiwan for earthquake observation. The study area includes a total of 169 stations managed by the Taiwan Strong-Motion Instrument Program (TSMIP) (Kuo et al., 2012). The distribution of these TSMIP stations is shown in Fig. 1. In this study, the peak ground acceleration (PGA) and peak ground velocity (PGV) obtained from seismographs are compared and analyzed. The ground motion data can be separated into three directions, namely the NS, EW, and vertical directions. To obtain the PGA and PGV in the horizontal plane and three-dimensional space, combinations of ground motion in the NS-EW directions and in all three directions were calculated, respectively, and then the PGA and PGV were assessed.

2.4. Hydrological monitoring networks

The hydrological observation data used in this study include precipitation, river discharge, and groundwater level. The distribution and number of monitoring stations are shown in Fig. 1 and listed in Table 1. The groundwater level monitoring system adopted in this study include devices managed by the WRA (referred to as WRA wells), which have a sampling interval of 1 h, devices managed by the GSMMA (referred to as GSMMA wells), which have a sampling interval of 10 min, and devices managed by the CWA (referred to as CWA wells), which have a sampling interval of 1 s. There are 176 and 139 WRA wells in Chianan and Pingtung plains, respectively; however, only 122 and 125 of the wells, respectively, recorded data for the Meinong earthquake due to device or well problems. There are only six CWA wells in Taiwan (see Table 2 and Fig. 1), three of which are located in the study area. The CWA wells were chosen based on the WRA wells, which have high sensitivity for detecting groundwater level anomalies triggered by earthquakes (Lai et al., 2010). However, the CWA wells are newly constructed wells, different from the WRA wells, with high-resolution monitoring devices. Therefore, although the CWA and WRA wells are almost collocated, they are not the same wells. GSMMA started installing observation wells for groundwater resource investigations in mountainous areas in Taiwan in 2010. There are 14 GSMMA wells at seven locations near the study area (see Table 3 and Fig. 1). Each location has two wells opened at different depths within 100 m. Chianan and Pingtung plains have a total of ten and six river gauge stations, respectively (Fig. 1). The watershed pattern is different in these two areas; it is commonly a parallel drainage system in Chianan Plain and a dendritic drainage system in Pingtung Plain. Because the variations in river discharge and groundwater level are largely affected by rainfall quantity, precipitation data are used to confirm the hydrological conditions during the observation period. From the precipitation stations distributed in the study area, four and five were selected in Chianan and Pingtung plains, respectively, to confirm the influence of precipitation on river discharge and groundwater level. The rainfall data are shown in time series figures to compare hydrology in the following section.

Table 2
Information on CWA wells and groundwater level variations triggered by Meinong earthquake.

Well	Screen depth (m)	Epicentral distance (km)		Step GWL variation (m)	Oscillation GWL amplitude (m)
		EQ1*	EQ2*		
Naba	135–147	26.48	16.36	1.110	2.222
Chishan	158–170 182–197	37.02	48.99	–	0.059
Liujar	204–222	39.69	27.55	0.010	0.366
Donher	222–252	83.2	72.42	–	0.205
Hualien	140–160	160.04	155.72	–	0.088
Tunwei	130–150	239.06	232.5	0.007	0.029

GWL: groundwater level.
* EQ1 and EQ2 are the epicenters of the first and second earthquakes, respectively, proposed by Lin et al. (2018).

WRA wells are the main target of this study due to their uniform distribution. The horizontal distance between wells is around 5 km. A single location can include one to five wells with screens opened at different depths. The well number indicates the order (in terms of depth) at a given location, from shallow to deep (not the aquifer number). For example, Hsinhua 1 is opened at a shallower depth than that of Hsinhua 2. The wells are not uniformly distributed in different aquifers. The deepest aquifer commonly has the fewest observation wells, which makes comparisons at different depths difficult. Note that the observed groundwater level for a CWA well is a relative level (with respect to an initial value), whereas that for a WRA and GSMMA wells are an absolute level (with respect to the mean sea level).

During the earthquake occurrence, the rainfall quantity was insignificant, which is in the dry season in southern Taiwan. Therefore, the natural drivers of changes in river discharge and groundwater level during the observation period should be mainly due to the Meinong earthquake. Other natural factors that can affect groundwater level are the periodic variations due to sea, Earth, and barometric tides. The influences of anthropogenic activities are difficult to quantify. For example, farmers in the study area commonly pump groundwater for paddy field irrigation from January 15 to February 15, but the pumping quantity is unknown because the groundwater management strategies are not well developed and executed (Wang et al., 2015a, b; Wang, 2015). Therefore, the influence of groundwater pumping is the main uncertainty in the observation data.

3. Hydrological observations during Meinong earthquake

The main purpose of this study is to investigate the mechanism of groundwater responses in alluvial plains due to the Meinong earthquake. WRA wells are uniformly distributed in the study area and are thus the main data source for the analysis. Groundwater observations from the GSMMA and CWA wells and river discharge and rainfall data are used to validate the previously proposed mechanisms for groundwater responses in the WRA wells. For data from the CWA wells, the hydroseismogram for the six wells are shown with the distance distribution for comparison. For data from the GSMMA wells, observations at

Table 1
Number of observation stations used in this study.

Area	Number of observation stations					
	Groundwater level wells			Strong motion stations	River discharge gauges	Precipitation stations
	WRA	CWA	GSMMA			
Chianan Plain	176	2	–	106	10	4
Pingtung Plain	139	1	–	63	6	5
Mountain region	–	–	14	–	–	–

WRA: Taiwan Water Resources Agency; CWA: Taiwan Central Weather Administration; GSMMA: Taiwan Geological Survey and Mining Management Agency.

Table 3
Information on GSMMA wells and groundwater level variations triggered by Meinong earthquake.

Well no.	Well	Screen depth (m)		Epicentral distance (km)		Step GWL variation (m)	
		Shallow	Deep	EQ1*	EQ2*	Shallow	Deep
B104W-01	Gaozhong	20–32	76–88	30	26	0.098	0.010
B104W-02	Baolong	27–39	79–91	15	9	−0.525	–**
B104-03	Dalin	16–28	72–84	5	7	−0.359	3.191
B104W-04	Guanglin	17–29	64–67 76–79 85–91	6	14	0.017	0.069
B104W-05	Liugui	30–42	85–97	11	17	0.044	0.006
B104W-06	Maolin	18–30	67–76 91-94	15	23	–	–
B104W-07	Sandimen	20–32	70–76 85-91	27	39	0.025	0.027

GWL: groundwater level.
* EQ1 and EQ2 are the epicenters of the first and second earthquakes, respectively, proposed by Lin et al. (2018).
** "-" indicates no observation data.

different depths at a given location are shown for comparison. For data from the WRA wells, because groundwater level oscillation is not easily detected and unsuitable for analysis, the values of step changes in groundwater level are adopted. River discharge data were examined and only five stations showed anomalies.

WRA wells sample on the hour. Therefore, the defined coseismic responses of groundwater level are at 4:00 (the Meinong earthquake was at 3:57). Note that the first response record is the groundwater level around 2 – 3 min after the Meinong earthquake. If the disturbance caused by the Meinong earthquake was not large or if the

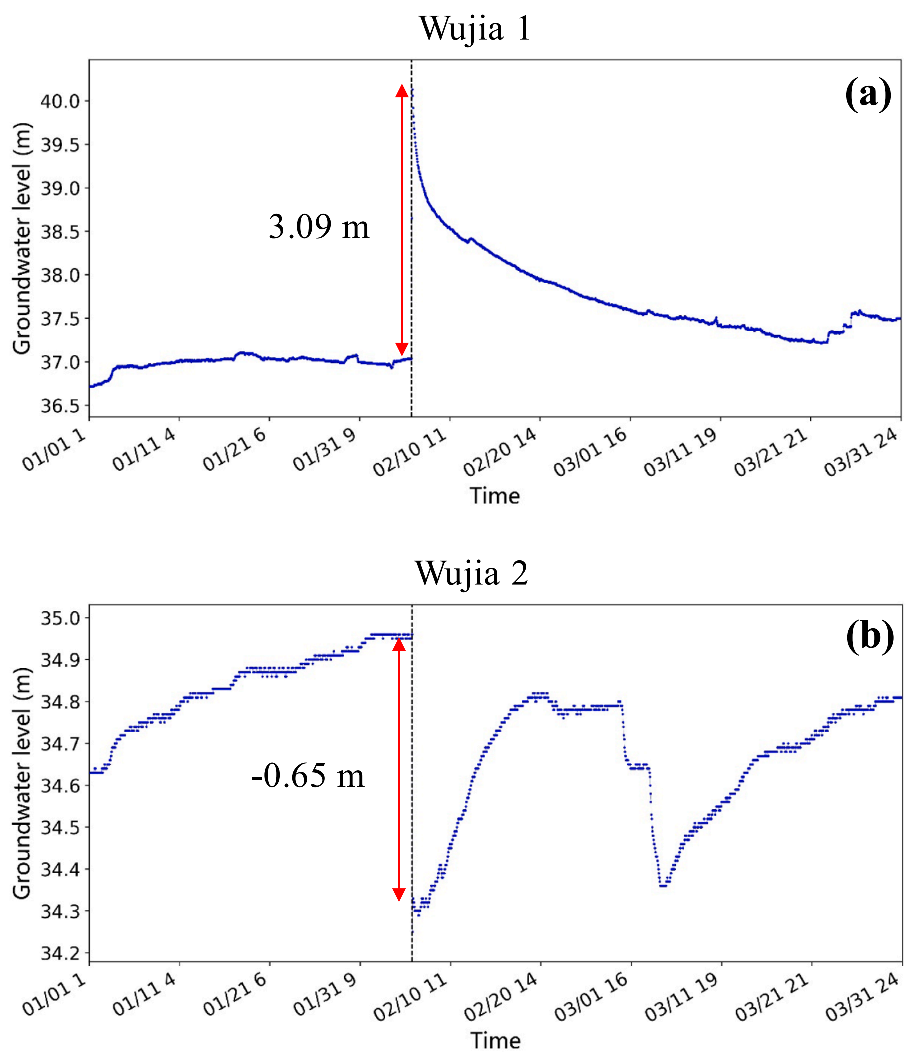

Fig. 3. Examples of calculation of step change in groundwater level in WRA well at (a) Wujia 1 and (b) Wujia 2. Vertical dashed lines mark the occurrence time of the Meinong earthquake. Red double arrows mark the definition of step change in groundwater level. (For interpretation of the references to color in this figure legend, the reader is referred to the web version of this article.)

hydrogeological properties made the aquifer highly drainable, changes in groundwater level might not have been recorded. The definition of step changes in groundwater level for the hourly sampling interval adopted in this study is based on the groundwater levels before and after the occurrence of the earthquake having a recognized shift (>0.01 m). The step quantity is calculated as the maximum (or minimum if the level decreased) quantity of the groundwater level within two time steps (i.e., data between 4:00 – 5:00 in this study) after the occurrence of the earthquake minus the level just before the occurrence time of the earthquake (at 3:00). Two examples for Wujia station at different depths are shown in Fig. 3. After the earthquake, the groundwater level at Wujia 1 reaches a maximum value and then continuously decreases. The step change is calculated as the maximum value minus the level before the earthquake. The groundwater level at Wujia 2 had a significant decrease after the earthquake, followed by a gradual decrease, with the minimum value reached after around 7 h. Since the gradual change might have been caused by other factors (e.g., a water sink or source), it is not considered in the defined coseismic responses. Therefore, the step change in groundwater level is calculated as the minimum value during 4:00 – 5:00 minus the level before the earthquake. Three classes of step magnitude, namely <0.05 m, 0.05 – 0.30 m, and >0.30 m, are used to show the pattern of spatial distribution, based on the quantities of the step changes in groundwater level triggered by the Meinong earthquake. The assessment results for each well are provided in the Supplementary

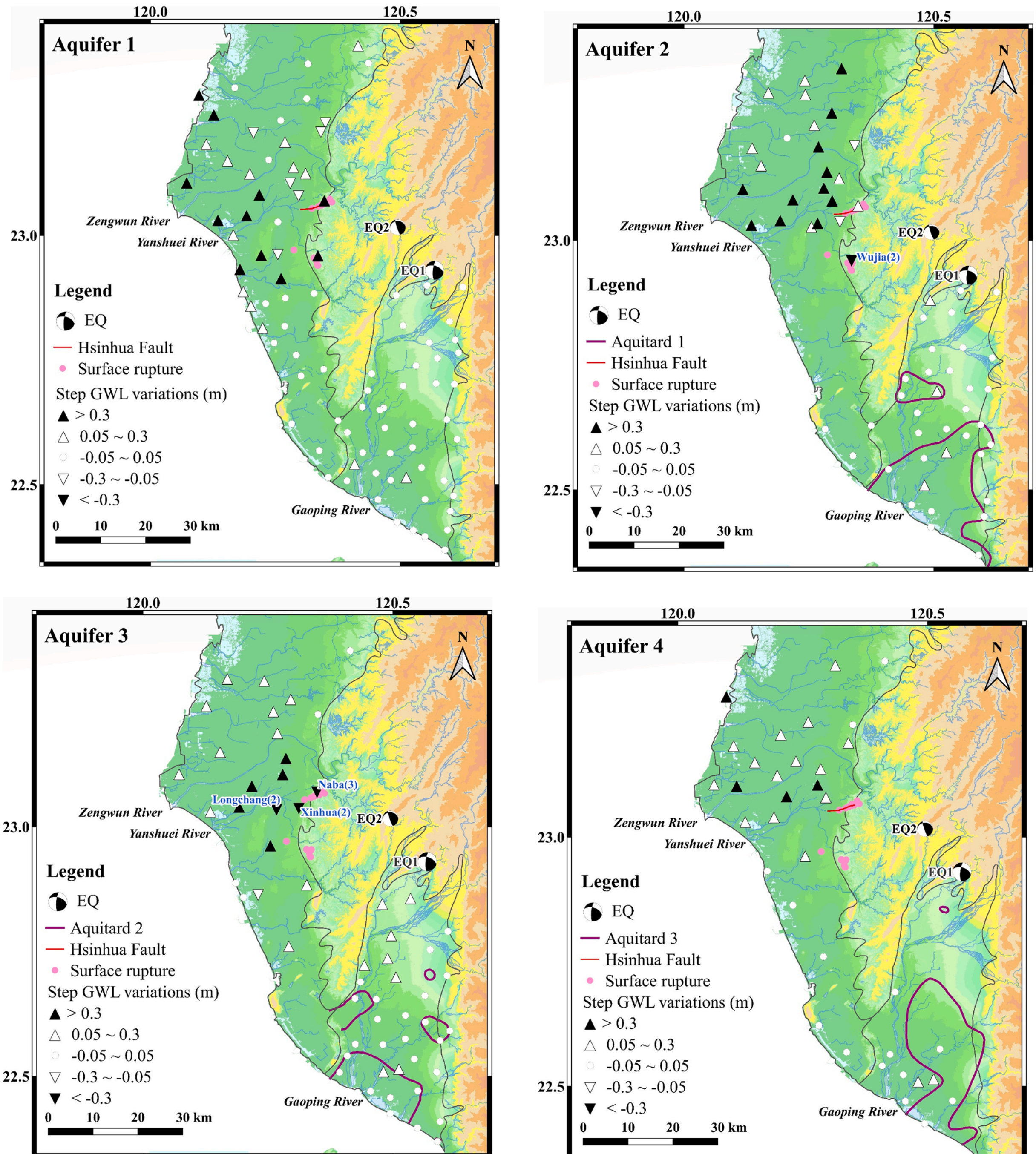

Fig. 4. Distribution of step groundwater level variations triggered by Meinong earthquake in aquifers (a) 1, (b) 2, (c) 3, and (d) 4. Purple lines delineate the aquitard distribution above the aquifers in Pingtung Plain. Black lines delineate the plain areas. (For interpretation of the references to color in this figure legend, the reader is referred to the web version of this article.)

Material.

3.1. Spatial distribution of step changes in groundwater level

Fig. 4 shows the distribution and Table 4 lists the statistical results of the step changes in groundwater level for WRA wells triggered by the Meinong earthquake in various aquifers in Chianan and Pingtung plains. Most of the step changes in groundwater level triggered by the Meinong earthquake are increases. The obvious step changes in groundwater level (defined as change larger than 0.3 m) are mainly located in Chianan Plain. The groundwater level at most of the wells in Pingtung Plain did not show obvious responses; only 16 wells show a small increase (0.05 – 0.30 m). Only four and nine wells in Chianan Plain show obvious and small step decreases in groundwater level, respectively. The no changes (defined as changes smaller than 0.05 m) in groundwater level might be due to 1) the groundwater level actually not having a response or 2) the variations in groundwater level recovering to the original level in a short period of time (and thus were not recorded by the device around 2 – 3 min after the Meinong earthquake). The observation data obtained at a 1-Hz sampling interval indicate that even the Tunwei and Hualien wells (shown in the inset figure in Fig. 1), which are far away from the epicenter, showed oscillation (Fig. S1). Therefore, the second cause is more likely.

Besides the planned distribution of the step change in groundwater level, a comparison between the step changes in groundwater level and the observation depths for each well was shown in Fig. 5. From the results, step changes in groundwater level and observation depths do not show any correlation but rather a decreasing pattern. The reason could be that observation depth does not have a clear physical mechanism connecting it to the step change in groundwater level but rather to the hydromechanical properties. In general, the particles in an aquifer are relative loose at shallow depths and relative dense at deep depths. A loose aquifer is more susceptible to disturbances that can induce a larger step change in groundwater level. However, a heterogeneous aquifer system affects the quantities of step change in groundwater level at various depths. Accordingly, the step change in groundwater level does not exhibit a clear relationship with depth but rather shows a decreasing pattern.

3.2. Groundwater hydroseisms and short-term fluctuations

Fig. S1 shows the observed groundwater level variations in the CWA wells with a 1-Hz sampling interval. The results show that during the earthquake period, oscillations in the groundwater level were obvious in all wells, but only the Naba, Liujia, and Tunwei wells showed step changes in groundwater level (111, 1.0, and 0.7 cm, respectively), as listed in Table 2. The Tunwei well, located 239 km away from the epicenter of EQ1 (Fig. 1), showed very small step changes in groundwater level. These changes were detected and separated in the time series. From Wang and Manga (2010), static stress and strain commonly occur in the near field, defined as the distance within one fault length. Therefore, the result implies that static stress is too far away to be the mechanism to triggered the step change at Tunwei well. The Tunwei well is the most sensitive well among the six CWA wells used for observing step groundwater level anomalies (Wang et al., 2015c).

Table 4
Number of wells with step change in groundwater level in Chianan and Pingtung plains.

Plains	Range of step changes in groundwater level (m)				
	Obvious decrease	Small decrease	No change	Small increase	Obvious increase
	< −0.30*	−0.30 to −0.05	−0.05 to 0.05	0.05 to 0.30	> 0.30
Chianan	4	9	33	45	31
Pingtung	0	0	109	16	0

* Step change in groundwater level was calculated as post-seismic level minus pre-seismic level.

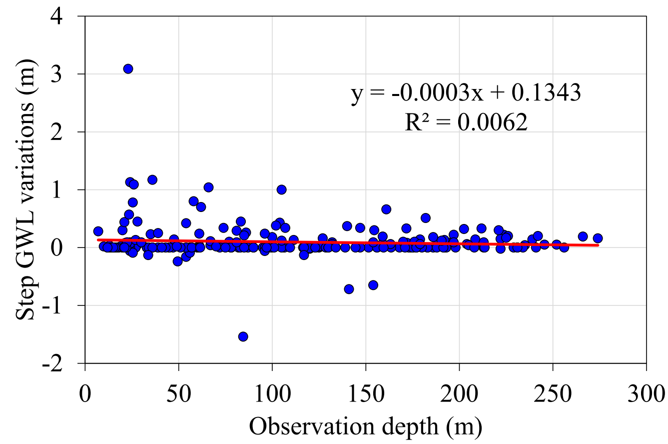

Fig. 5. Scatter plot of the step change in groundwater level with the observation depth. Note that not all observation wells have screen opening information (GWL: groundwater level).

3.3. Groundwater level in mountainous areas

Fig. S2 shows the observed groundwater level variations in mountainous areas. Due to the limitations of drilling machines, the wells were mainly installed in a relatively flat area with agricultural activity. Therefore, the groundwater levels have significant fluctuations due to human activity. During the Meinong earthquake, most of the wells recorded groundwater level anomalies, as listed in Table 3. Some responses were large and thus easily recognized but some responses were small, requiring a magnified view for analysis. The groundwater level in the deep well at Dalin station shows very large increases that correspond to decreases at the shallow depth. Because these wells are mainly installed in a rock system, the mechanism of groundwater level variations triggered by the Meinong earthquake might be different from that of those in a plain area. There is no significant pattern of the step changes in groundwater level with respect to epicentral distance.

3.4. River discharge anomaly

An increase in river discharge is a commonly observed anomaly triggered by earthquakes. Data from river gauge stations for the rivers in Chianan and Pingtung plains were checked. Only four stations in Chianan Plain (Hsinchung 1, Tsochen, Erhchi Bridge, and Hsinshin) and one station in Pingtung Plain (Shanlin Bridge 2) showed anomalous variations due to the Meinong earthquake, as shown in Fig. S3. River discharge anomalies were observed in a small area in the southern rivers of Chianan Plain. In Pingtung Plain, the only river discharge anomaly was observed in the upstream of Gaoping River. This might be due to the coseismic shaking being small (Lin et al., 2018) and the watershed and flow rate being relatively large in Pingtung Plain. The magnitude of the Meinong earthquake might not have been large enough to induce a huge increase in river discharge. Any increase in river discharge due to the Meinong earthquake would have been small relative to the river discharge and hence would be difficult to observe. Conversely, the coseismic ground shaking was large and the watershed and flow rate were small in Chianan Plain, where the river discharge anomalies were thus relatively easy to observe.

4. Mechanism validation and Discussion

The mechanism of groundwater level variations triggered by earthquakes can be separated into intrinsic factors and driving factors. The former include the sensitivity of aquifer response to earthquakes, such as volumetric strain sensitivity (Roeloffs, 1996). However, the resolution of hourly groundwater level data collected in this study is insufficient for calculating the volumetric strain sensitivity. Transmissivity is the ability of an aquifer to transmit groundwater in the horizontal direction and confinement constrains the vertical dissipation ability for excess pore water pressure (Freeze and Cherry, 1979). These two passive properties maintain the change in groundwater level triggered by earthquakes and are thus compared with the step changes in groundwater level. The driving factors include the change in static and/or dynamic stress due to earthquakes (Wang and Manga, 2010, 2021). Static stress can be assessed using the focal mechanism or the stress-–strain model (e.g., dislocation model or Coulomb stress model). Dynamic stress is caused by seismic waves. Both static stress and dynamic stress are discussed in regard to the step changes in groundwater level. Note that intrinsic properties may change during an earthquake, inducing changes in the groundwater level.

In this section, several mechanisms were validated and discussed. First, the distance effect and the static stress–strain mechanism that induces groundwater responses are checked. Second, the mechanism of ground-motion-induced groundwater responses is checked. Third, the confinement and transmissivity data are compared to determine the drainage effect on groundwater responses. Fourth, the mechanism of the step changes in groundwater level at multi-depth wells is discussed. Finally, the overall mechanism that induces the step changes in groundwater level during the Meinong earthquake is summarized.

4.1. Static stress–strain mechanism

Based on the static stress–strain concept, step increases and decreases in groundwater level are due to compressive and tensile stresses,

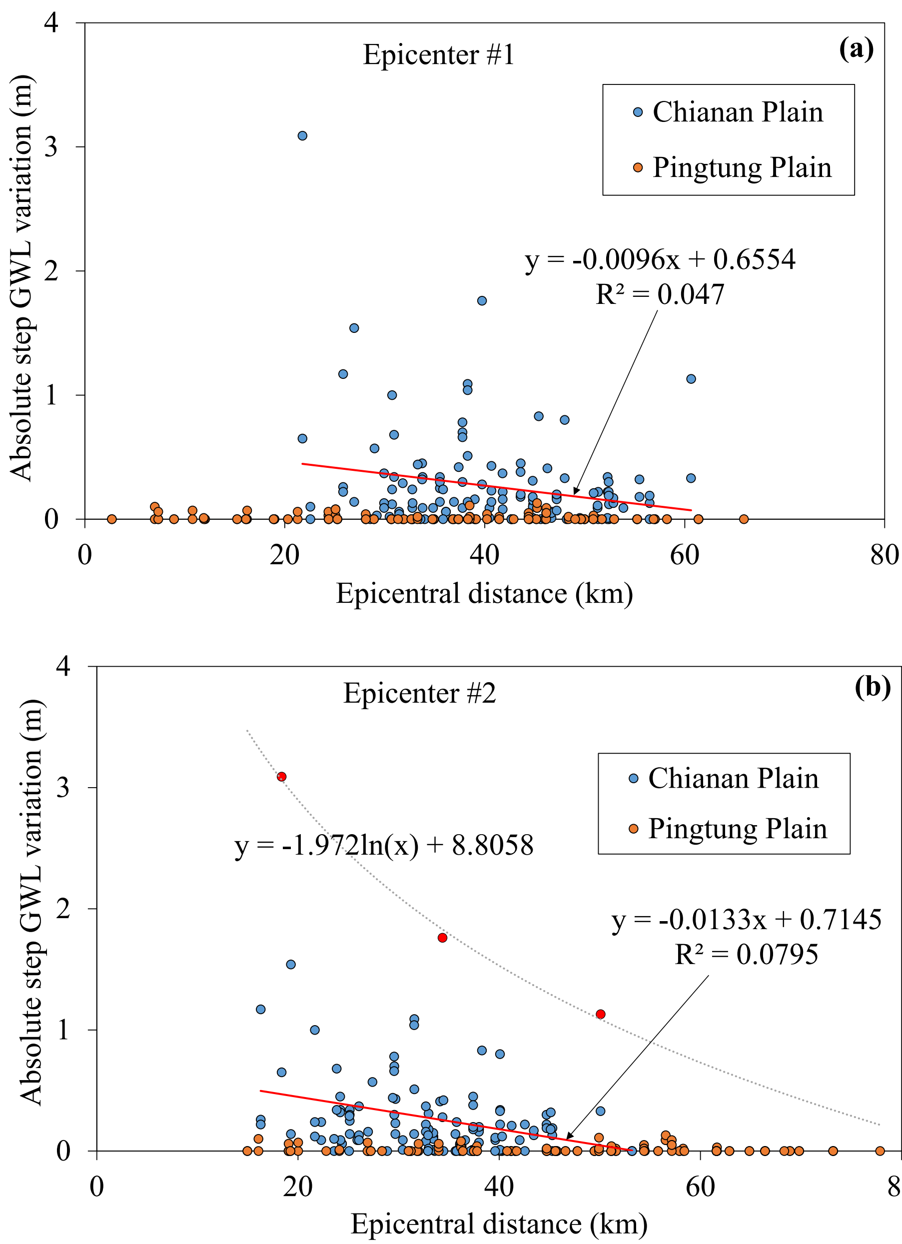

Fig. 6. Relationship between absolute step changes in groundwater level and epicentral distances for epicenters of (a) first and (b) second earthquakes. The linear regression curves were fitted to the data for Chianan Plain. The natural-log regression curve in (b) is the upper limit of the data for Chianan Plain fitted to the three red points using the epicenter of the second earthquake (GWL: groundwater level). (For interpretation of the references to color in this figure legend, the reader is referred to the web version of this article.)

respectively (Wang and Manga, 2010, 2021). From the focal mechanism of EQ1 (shown in Fig. 1), the compression areas are the northwest and southeast areas and the tension areas are the northeast and southwest areas. The Coulomb stress simulation results for the Meinong earthquake reported by Wen et al. (2017) show that the compression stress within a depth of $0-10$ km was distributed near Hsinhua Fault (Fig. 1). Most of the groundwater level responses in the compression area are increases, matching the stress–strain condition. However, although Pingtung Plain is located in the tension area, no groundwater level decrease was observed. In addition, neither the focal mechanism nor the Coulomb stress model can explain the step increases and decreases in groundwater level at different depths observed at a given location. These results indicate that the behavior of the groundwater level responses in sedimentary media during the Meinong earthquake cannot be described using the static stress–strain physical model with the epicenter or fault geometry. Note that Hsinhua Fault is not the fault that induced the Meinong earthquake but the location where the surface rupture and soil liquefaction were observed.

The mechanisms of step changes in groundwater level triggered by earthquakes are commonly discussed using near, intermediate, and far field concepts (Wang and Manga, 2010; Manga and Wang, 2015). However, from the observations in this study, the groundwater level responses did not decrease with increasing distance from the epicenter; instead, they showed large variations with epicentral distance. A blind fault induced the Meinong earthquake, so no fault distance can be used in the assessment. With an ideal poroelastic mechanism in a two-dimensional system, the force attenuates with an increase in the squared distance from a point source (Wang et al., 2015c). The relationship between the absolute step changes in groundwater level and the epicentral distance is shown in Fig. 6 for the two epicenters proposed by Lin et al. (2018). The linear regression equations fitted to the data for Chianan Plain are shown in the figure. The results indicate that the responses of groundwater level do not have a significant relationship with epicentral distance, as only a decrease pattern can be observed.

The upper limit of the data for Chianan Plain fitted to the three red points shown in Fig. 6b can be written as:

$$Step_{abs} = -1.972 \times \ln(d) + 8.8058 \tag{1}$$

where $Step_{abs}$ is the absolute step changes in groundwater level in meters and d is the epicentral distance from the epicenter of EQ2 in kilometers. This equation provides the upper limit for the step groundwater level response induced by the Meinong earthquake within a certain distance.

The groundwater level responses in Pingtung Plain were very small and do not show a clear pattern with epicentral distance whereas those in Chianan Plain were large and show a decreasing pattern (Fig. 6), even though these two plains are located at similar epicentral distances. This difference can be due to differences in intrinsic and driving factors. Note that if the unchanged groundwater level responses are considered, the decreasing pattern becomes unclear. The unchanged groundwater level implies a zero response, which is important information for the analysis and should not be ignored. Furthermore, the step changes in groundwater level were increases and decreases at different depths at a given location, which increases the uncertainty in constructing the empirical relationship between the step changes in groundwater level and epicentral distance. Therefore, the empirical relationship between the step changes in groundwater level and epicentral distance (e.g., King et al., 1999; Matsumoto et al., 2003; Roeloffs, 1998; Wang et al., 2015c) obtained without considering other factors may have large uncertainty and should be carefully considered.

4.2. Ground motion effect

It has been reported that step changes in groundwater level and liquefaction have a higher correlation to PGV than to PGA (e.g., Midorikawa and Wakamatsu, 1988; Wang et al., 2006; Wong and Wang, 2007). A large amount of soil liquefaction (including sand eruption and soil boiling phenomena) was observed in Chianan Plain during the Meinong earthquake. Soil liquefaction occurs when the excess pore water pressure is equal to or greater than the total stress. PGA and PGV in different directions are compared with the step changes in groundwater level and liquefaction locations in the first aquifer to determine whether dynamic ground motion triggered the step changes in groundwater level.

The distribution comparisons between each direction of PGA and PGV and the step changes in groundwater level show that the horizontal PGV, a combination of the NS-WE directions, and the step changes in groundwater level have the most similar patterns (Fig. 7a). For comparison, the relation between horizontal PGA and the step changes in groundwater level is also shown (Fig. 7b). The soil liquefaction locations identified by the Disaster Prevention Research Center, National Cheng Kung University (Central Geological Survey, 2016), and the surface rupture points (not fault rupture) from the field survey conducted by the Graduate Institute of Applied Geology, National Central University (Le Beon et al., 2017), are also shown in the figure. The quantities of horizontal PGA and PGV are small in Pingtung Plain and large in Chianan Plain. From the horizontal PGV comparison (Fig. 7a), the wells with small decreases in groundwater level are mainly located in the area with low horizontal PGV and those with obvious increases in groundwater level are mainly located in the area with high horizontal PGV. The results show that the distribution of step changes in groundwater level is consistent with that of horizontal PGV but not significantly related to horizontal PGA, which is consistent with previous studies (e.g., Midorikawa and Wakamatsu, 1988; Wang et al., 2006; Wong and Wang, 2007).

The quantified relationships between step changes in groundwater level in the first aquifer and horizontal PGV and PGA, respectively, are shown in Fig. 8. The values of PGA and PGV were calculated using kriging interpolation to the location of the groundwater observation wells. The linear regression curve shows that the R-squared value (where R is the Pearson correlation coefficient) between step changes in groundwater level and horizontal PGV is higher than that between step changes in groundwater level and horizontal PGA, though both values are small. The R-squared values are small because all the zero groundwater level responses were considered and not all factors were considered. A non-response is important for representing the hydrogeological properties and thus should be included in the analysis. If a logarithmic scale is used for the step changes in groundwater level (following Wong and Wang, 2007), which means that only the positive step changes in groundwater level are considered, the correlation coefficient between the step changes in groundwater level and horizontal PGV is above 0.6 (R-squared > 0.36) (see Supplementary Material, Fig. S4), indicating a strong correlation (Dancey and Reidy, 2017). However, removing the zero responses also eliminates the threshold of the minimum horizontal PGV and PGA required to trigger groundwater level changes, leading to a loss of important information.

The small correlation may be due to the following. 1) The responses of an aquifer system to an earthquake are affected by its hydro-mechanical properties (e.g., volume strain sensitivity or natural frequency). A sensitive aquifer system can have a large response to seismic waves. The same PGA or PGV may trigger different step changes in groundwater level, thus decreasing the correlation between them. 2) The defined coseismic step change in groundwater level is around $2-3$ min after the earthquake. The actual quantity of coseismic step change in groundwater level might not have been completely detected in the hourly data. Consequently, the step change in groundwater level may not highly correlate with its driving force. 3) A highly permeable medium leads to fast dissipation, further decreasing the groundwater level. Along with the hourly sampling interval, the defined coseismic step change in groundwater level in this study may be lower than the actual step change in groundwater level, thereby reducing the correlation between the step change in groundwater level and seismic factors. 4) The

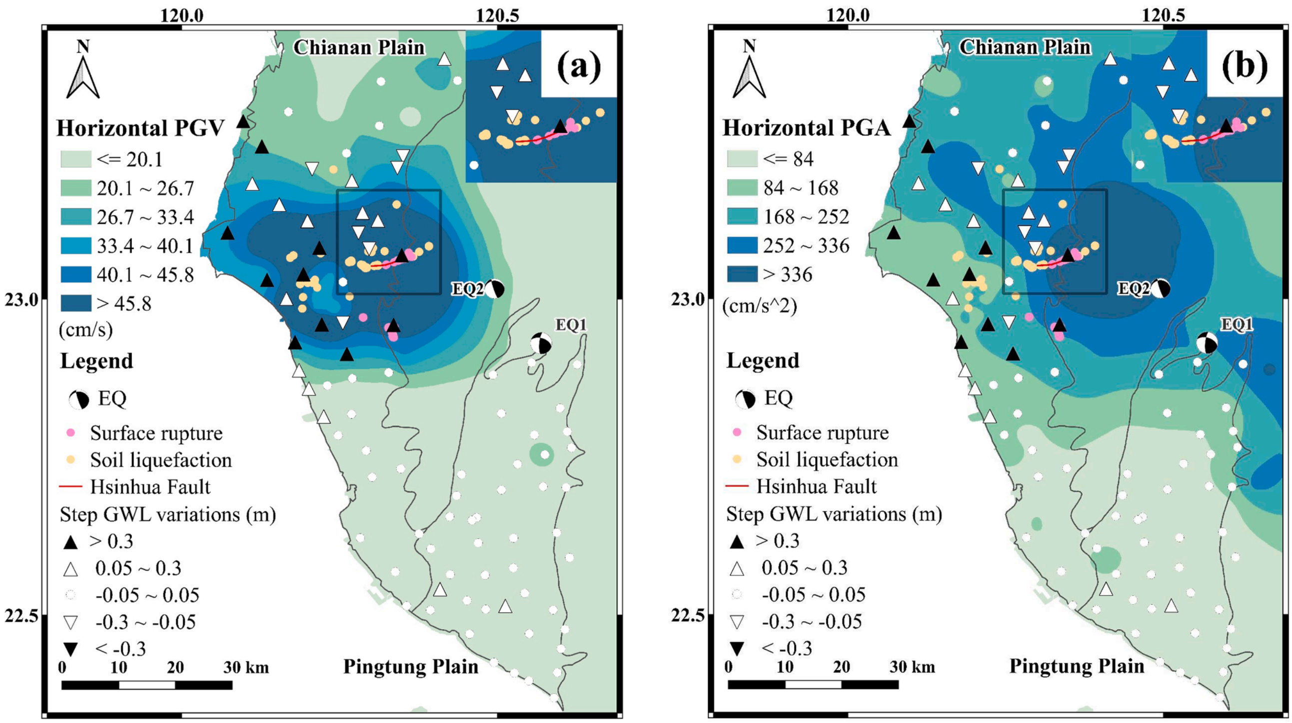

Fig. 7. Comparisons of horizontal (a) PGV and (b) PGA with surface rupture, soil liquefaction, and step changes in groundwater level in aquifer 1. The upper-right inset map is an enlargement of the rectangular area in the figure. The PGA and PGV data were provided by the Earthquake-Disaster & Risk Evaluation and Management Center (E-DREaM) at National Central University (Lin et al., 2018), and the soil liquefaction and surface fracture data were provided by the Disaster Prevention Research Center, National Cheng Kung University (CGS, 2016), and the Graduate Institute of Applied Geology, National Central University (Le Beon et al., 2017), respectively. Black lines delineate the plain areas (GWL: groundwater level).

comparison is based on the interpolation and extrapolation of the seismic factors to the groundwater wells. The seismic factors at the wells might not fully reflect the real situation, hence the correlation between the step change in groundwater level and seismic factors might not be high. Therefore, if we only consider the driving factors (seismic waves) without accounting for intrinsic factors (e.g., hydro-mechanical and hydraulic properties) and other conditions, the correlation will not be high. Nevertheless, dynamic stress is more consistent with the step changes in groundwater level than static stress. Dynamic stress may thus be the main driving force for the step changes in groundwater level triggered by the Meinong earthquake.

From Fig. 8a, the step changes in groundwater level and their uncertainty both increase with horizontal PGV. The uncertainty might be due to the aforementioned reasons. If a 0.3-m step change in groundwater level is defined as an obvious change, the minimum horizontal PGV that can trigger an obvious groundwater level change is around 25 cm/s. That is, when the horizontal PGV is lower than 25 cm/s, obvious groundwater level variations may not occur and most wells will show no change. When the horizontal PGV is larger than 25 cm/s, most of the wells will show a step change in groundwater level. The step changes in groundwater level and horizontal PGA do not show an obvious pattern, as shown in Fig. 8b. A minimum threshold of horizontal PGA can be defined as 120 cm/s^2. However, although the steps change in groundwater level approached zero when the horizontal PGA was lower than 120 cm/s^2, several wells showed no groundwater level response when the horizontal PGA was higher than 120 cm/s^2. Therefore, the definition of the minimum threshold of horizontal PGA is weak.

Dynamic shear stress–strain is known to be one of the main mechanisms that induce an increase in pore water pressure, even for a liquefaction event, during an earthquake (Holzer and Youd, 2007). Horizontal ground motion, not vertical ground motion, is the main factor that induces pore water pressure buildup (Yang et al., 2002). The results of the comparison between PGA and PGV directions with step changes in groundwater level in this study are consistent with this mechanism. The distribution of soil liquefaction shows a pattern similar to that of PGV (Fig. 7a), which is similar to the groundwater level changes at a shallow depth. The obvious increase in groundwater level has the same mechanism as that of soil liquefaction. Therefore, soil liquefaction events are also compared with horizontal PGA and PGV using kriging interpolation to the liquefaction point, as shown in Fig. 8c. There is a threshold for the minimum horizontal PGV and PGA required to induce soil liquefaction (40 cm/s and 160 cm/s^2, respectively).

Based on the results in Fig. 8, the minimum horizontal PGV required to induce a step change in groundwater level is 25 cm/s and that required to induce soil liquefaction is 40 cm/s. Even though horizontal PGA does not show good agreement with the step changes in groundwater level, the figure shows that the approximate minimum horizontal PGA required to induce a step change in groundwater level is 120 cm/s^2 and that required to induce soil liquefaction is 160 cm/s^2. These results are slightly different from those reported by Midorikawa and Wakamatsu (1988) and Wong and Wang (2007). The former study reported that the critical values for soil liquefaction for PGV and PGA are 10 – 20 cm/s and 70 – 250 cm/s^2, respectively, for several earthquake events in Japan. The latter study showed that the minimum PGV and PGA required to induce a step change in groundwater level are around 20 cm/s and 50 cm/s^2, respectively, for the 1999 Chi-Chi earthquake in Taiwan. The PGV results are in the same range whereas the PGA results show a large discrepancy. The PGV required to induce a step change in groundwater level and soil liquefaction might be independent of the area and earthquake event.

4.3. Hydrogeological effect

From the hydrogeological profile, the hydrogeological materials in Chianan and Pingtung plains have a large difference, which may be one of the reasons for the significantly different groundwater responses

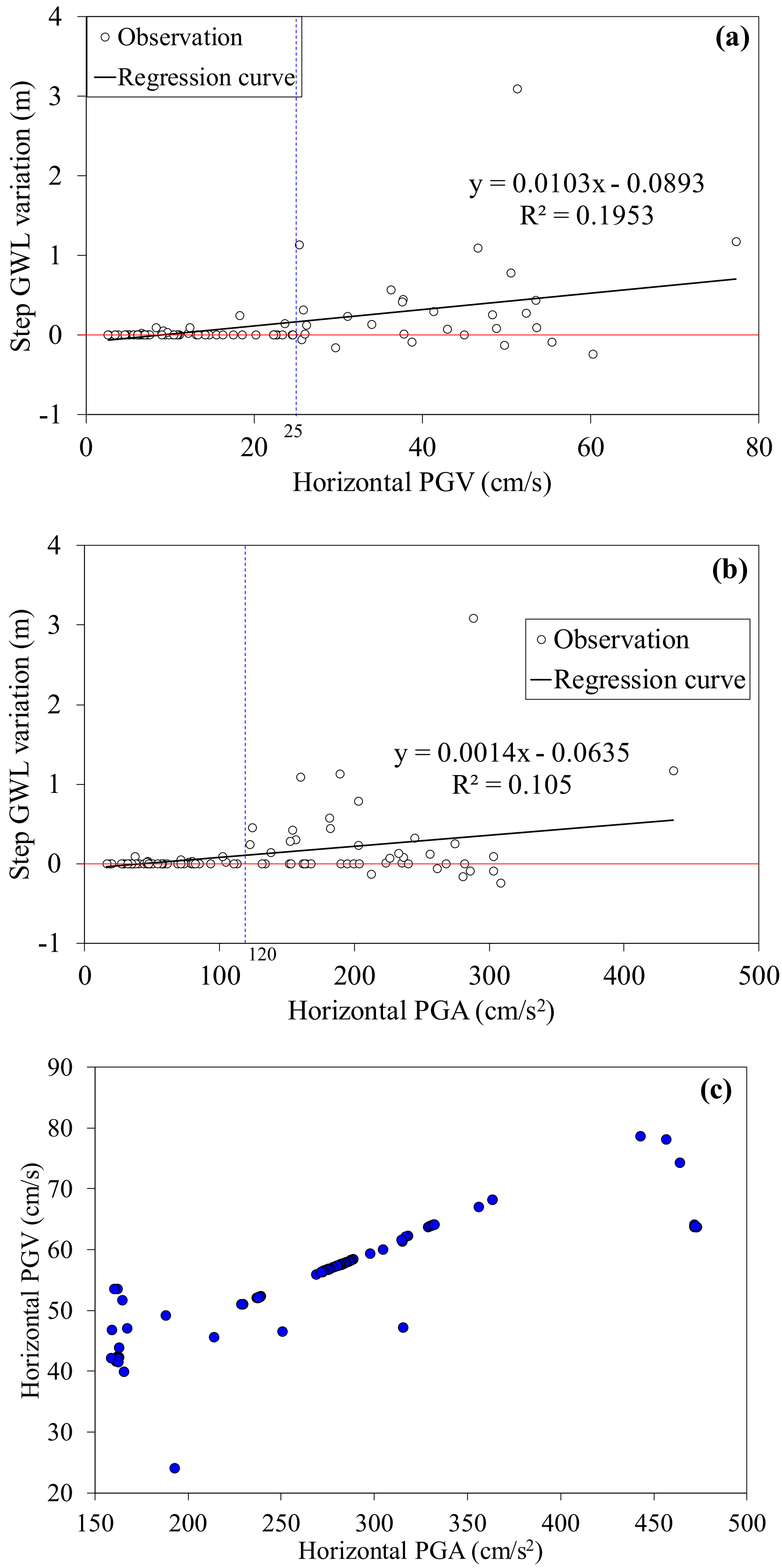

Fig. 8. Scatter plot between step changes in groundwater level and (a) horizontal PGV and (b) horizontal PGA and their minimum values required to trigger step changes in groundwater level. (c) Horizontal PGA and PGV at soil liquefaction points. Note that a single point in (c) actually has 1 to 46 liquefaction (eruption) events. Because these events are located in a small area, their PGA and PGV values are treated as being the same and only one point is shown. The total number of liquefaction points is 260. In (a) and (b), vertical line marks the minimum threshold and horizontal line marks the zero value (GWL: groundwater level).

triggered by the Meinong earthquake in these two areas. Transmissivity and confinement were collected and compared with the step changes in groundwater level to discuss the influence of hydrogeological properties.

The groundwater level response in Pingtung Plain, which is close to the epicenter, was lower than that in Chianan Plain, and half of the wells with responses are located in confined aquifers, as shown by the aquitard distributions in Fig. 4. The ground motion generated by earthquakes appears to be the driver of the induces changes in groundwater level. The hydraulic properties of an aquifer determine how long groundwater level changes persist. An aquifer with good confinement and/or small hydraulic conductivity (transmissivity) has a lower rate at which pore water pressure dissipates in the vertical and horizontal directions, respectively (Freeze and Cherry, 1979). Thus, the induced variations in pore water pressure persist for a relatively long period of time and are thus more easily detected by the piezometer during hourly sampling. In the unconfined aquifer, earthquake-induced groundwater level variations quickly dissipate, and are thus not easily detected. This explains why the step changes in groundwater level are small in aquifer 1 in Pingtung Plain. About half of the increases in groundwater level are consistent with the distribution of the above aquitard (Fig. 4), except for aquifer 3, where slightly increased step changes in groundwater level are mainly located in an area with small transmissivity (Fig. 9).

A comparison between the transmissivity and the step changes in groundwater level induced by the Meinong earthquake is shown in Fig. 10. The results show a negative trend between the step changes in groundwater level and transmissivity. Note that the step changes in groundwater level are not physically related to the quantity of transmissivity. An aquifer with higher transmissivity can dissipate excess pore water pressure faster and thus a lower groundwater level is expected. However, the quantity of excited pore water pressure depends on the properties of the aquifer response to earthquakes and the quantity

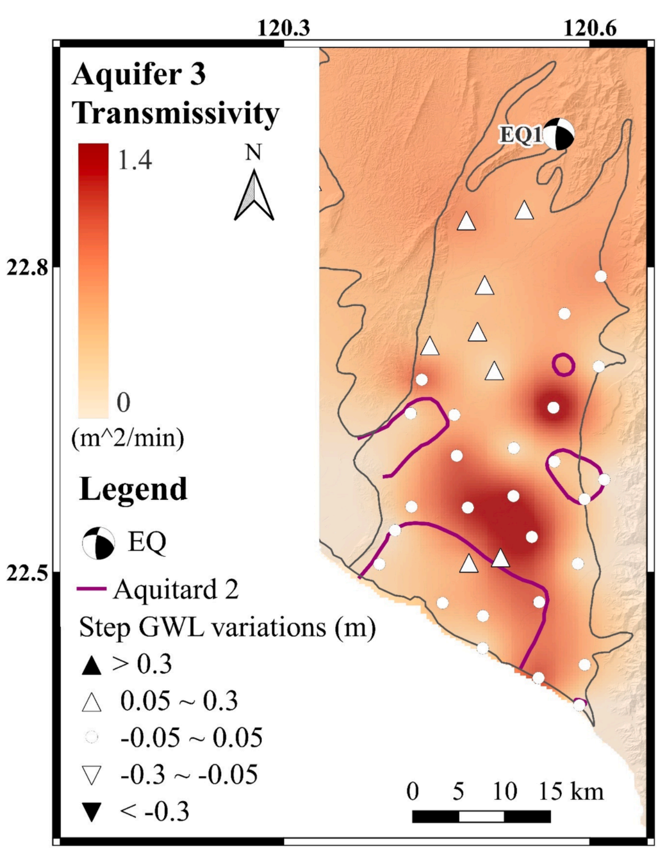

Fig. 9. Distribution of transmissivity in aquifer 3 in Pingtung Plain. Transmissivity data were collected from Central Geological Survey (2002).

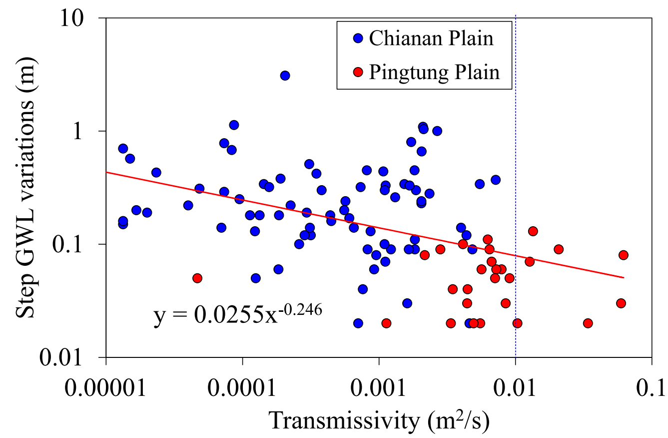

Fig. 10. Comparison between step changes in groundwater level and transmissivity. Transmissivity data were collected from Central Geological Survey (2002). Vertical line marks the threshold of significant step change in groundwater level (GWL: groundwater level).

of driving stress from earthquakes. Therefore, only the pattern between the step changes in groundwater level and transmissivity should be considered. Figs. 10 and S5 give an approximate threshold of transmissivity of 0.01 m^2/s. The step changes in groundwater level triggered by earthquakes were not easily observed in the hourly data when transmissivity was larger than 0.01 m^2/s. The transmissivity in Pingtung Plain is significantly larger than that in Chianan Plain, which is consistent with the step changes in groundwater level being smaller in Pingtung Plain.

4.4. Groundwater level variations in multi-depth wells

Of all the observation wells, only four showed an obvious step decrease in groundwater level. It is interesting that all four wells have a step increase in groundwater level at a shallow depth. The step changes in groundwater level at multiple depths show totally different behaviors at four locations, which results from a combination of different mechanisms at a given location at different depths. We discuss the possible mechanisms for these wells. Fig. 11 shows groundwater level anomalies at different depths of the WRA wells at the four locations. These responses can be separated into two groups. The first two figures show that the groundwater level in the deep aquifer is higher than that in the shallow one; the last two figures show the opposite situation. This means that for Naba and Hsinhua wells, there is potential for upward groundwater flow. The behavior at Wujia and Longchang wells is opposite, indicating the possibility of downward groundwater flow. The values of groundwater levels become close after the Meinong earthquake in the first group (i.e., the Naba and Hsinhua wells), and diverge in the second group (i.e., the Wujia and Longchang wells).

At all four locations, the groundwater levels in the deep aquifer show a decrease and those in the shallow one show an increase. All of these wells are located near the surface rupture area (Fig. 4). The post-seismic groundwater level did not return to the original level in a short period of time, which may imply that the aquifer properties or hydrological conditions changed. The increase in groundwater level could have been caused by the compression of pore water, additional water recharge, or both. The compression of pore water may be due to consolidation induced by dynamic shear strain or compression induced by static stress as the focal mechanism. For the mechanism of compression induced by static stress in a traditional two-dimensional concept, the groundwater level will not show both increases and decreases at a given location at different depths (within 250 m) (Shalev et al., 2016a, b). Therefore, the increase in groundwater level at the shallow depth of these four wells is likely due to pore water pressure buildup induced by dynamic shear

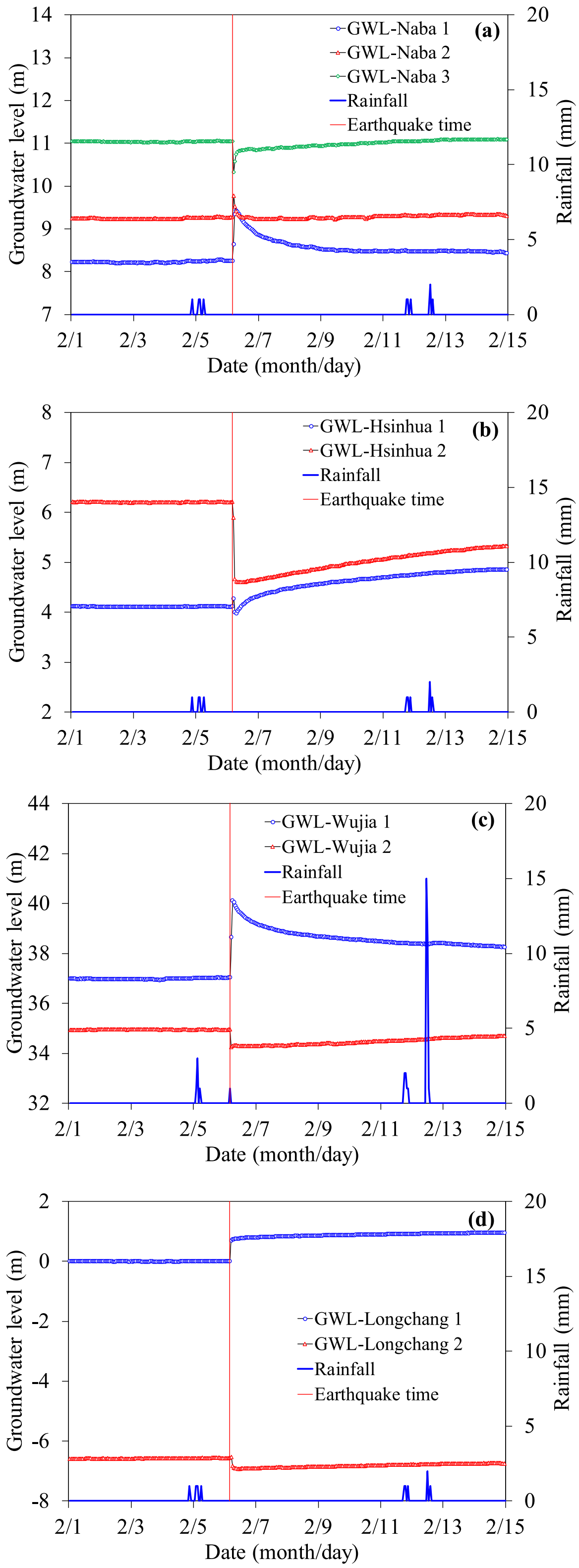

Fig. 11. Step changes in groundwater level at multiple depths for (a) Naba station, (b) Hsinhua station, (c) Wujia station, and (d) Longchang station triggered by Meinong earthquake in WRA well system. Vertical red line indicates the time of earthquake occurrence. The sampling interval is one hour. The number after the well name indicates the rank at a given location, from shallow to deep. For example, Naba 1 is opened at a shallow depth and Naba 2 is opened at a deep depth (GWL: groundwater level). (For interpretation of the references to color in this figure legend, the reader is referred to the web version of this article.)

strain for uncemented porous media or additional water recharge.

A decrease in groundwater level is known to be due to enhanced permeability induced by fracture opening or tension strain (Wang and Manga, 2010). The stress–strain mechanism was shown above to not match the observations. Permeability enhancement commonly occurs in a low-permeability material, such as an aquitard or partially or fully consolidated media. Enhanced permeability can be caused by the formation of pore spaces (e.g., consolidated media) or the construction of flow paths (e.g., aquitard material) for transmitting groundwater. The former directly decreases the groundwater level due to an additional volume of spaces. The latter allows water movement from an area with high hydraulic head to that with low hydraulic head, decreasing the groundwater level due to water discharge. Both mechanisms can occur in the four wells because the lithology of the deeper sediments is partially cemented (Fig. 12). Note that although the lithology is marked as bedrock in the rightmost red bar in Fig. 12a and 12b, the materials from the core sample were not fully consolidated and are also marked as sedimentary materials in the left color bar. There is no detailed hydrogeological information for Hsinhua and Longchang wells. As shown in Fig. 12c, these two wells are located near the Tainan tableland (Huang et al., 2009) or Toukoshan Formation and Terrance Deposits, and have lithology conditions similar to those for the Naba and Wujia wells. Most of the wells with a decrease in groundwater level in Fig. 12c have similar lithology conditions, namely loose sediments at a shallow depth and partially consolidated sediments at a deep depth. The stress–strain mechanism was shown to not match the observations. This indicates that the decreases in groundwater level may be mainly due to damage to partially consolidated materials, which is similar to the mechanism of permeability enhancement (Wang and Manga, 2010, 2021).

The groundwater levels increased in the shallow aquifer and decreased in the deep aquifer at four locations after the Meinong earthquake. The hydraulic heads at different depths at Naba and Hsinhua become similar and those at Wujia and Longchang diverged, unlike those discussed by Wang et al. (2016) who showed that the groundwater level become similar in different aquifers after the Taiwan Chichi Earthquake. The divergence also indicates that groundwater was not connected in the casing between different wells at different depths during the Meinong earthquake. The groundwater responses indicate that water at different depths was in different groundwater systems. The Meinong earthquake created paths that gave the pore water pressure potential to propagate from the deep aquifer to the shallow aquifer at some locations (e.g., Naba and Hsinhua wells), as discussed by Wang et al. (2017).

4.5. Summary of mechanisms

From the integrated observations discussed above, the step increase in groundwater level at a shallow depth may be mainly due to dynamic-shear-strain-induced compression or additional water recharge, and the step decrease in groundwater level at a deep depth may be mainly due to fracture opening or water discharge to other areas. The obvious step decreases are mainly located near the area of the surface rupture and partially cemented sediments, which indicates that the Meinong earthquake may have created new porous space and decreased pore water pressure. Therefore, the integrated observations made during the Meinong earthquake indicate that ground motion and hydraulic properties are important factors in hydrological anomalies in sedimentary media.

5. Conclusions

Hourly, 10-minute, and 1-Hz data of groundwater level variations triggered by the Meinong earthquake in Taiwan were collected and compared to the river discharge, ground motion, liquefaction, surface rupture, and previously reported results to validate the previously proposed mechanisms of groundwater response triggered by earthquakes. Data for two different hydrogeological conditions in regions to the west

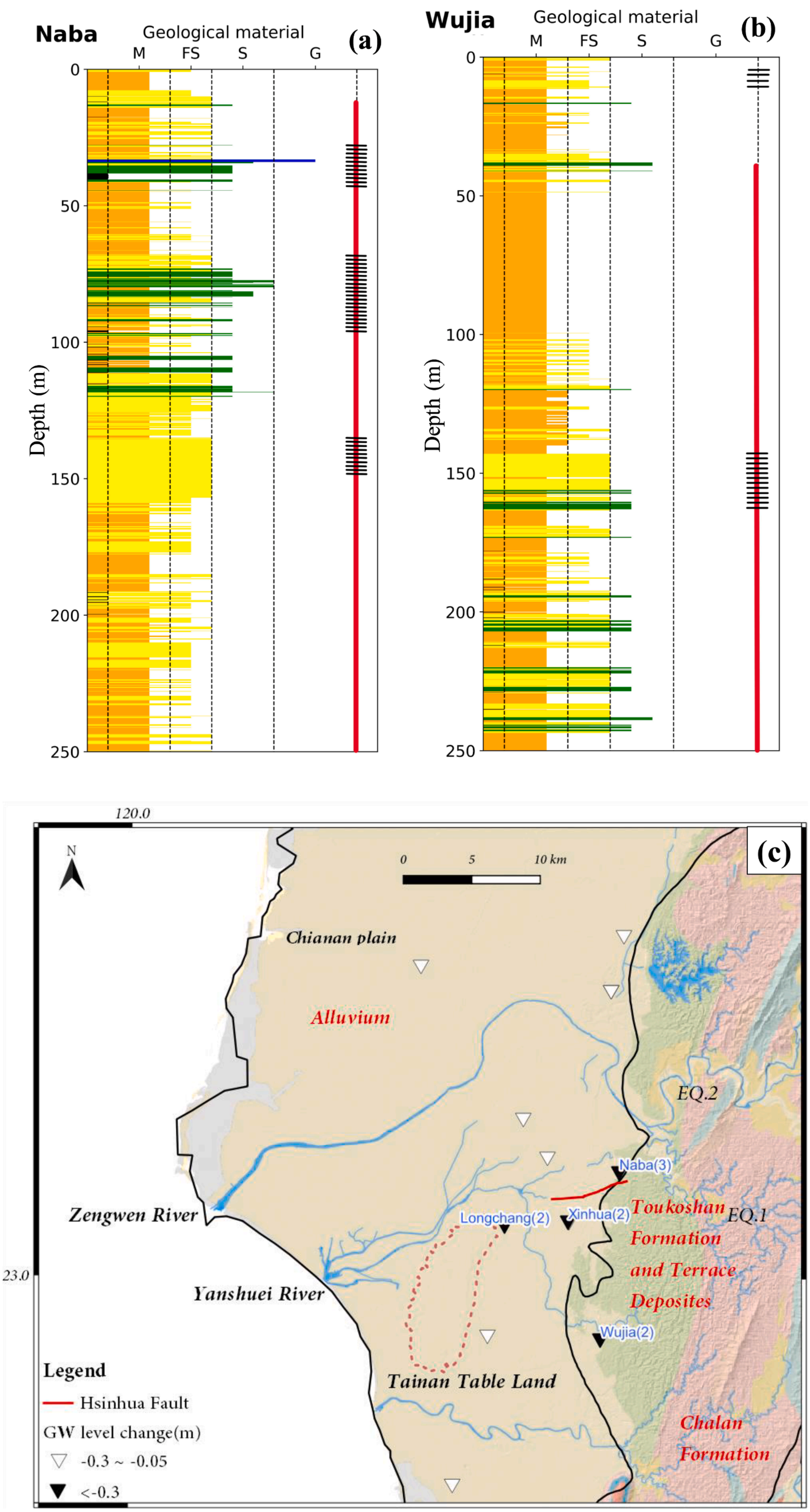

(caption on next page)

Fig. 12. Detailed hydrogeological materials at (a) Naba and (b) Wujia wells. Geological material in the log setting can be read from both color bar and top axis. Blue, green, yellow, and brown colors indicate gravel (G), coarse sand (S), find sand (FS), and Mud (M). The red bar on the right-hand side indicates the bedrock location defined by the GSMMA. The short horizontal lines on the right-hand side indicate the location of opened screens. (c) Geological map with distribution of decreases in groundwater level. Geology data were collected from Central Geological Survey (https://hydro.geologycloud.tw/ [in Chinese]). (For interpretation of the references to color in this figure legend, the reader is referred to the web version of this article.)

and south of the epicenter were compared. Most groundwater levels in the south region (Pingtung Plain), which is close to the epicenter, did not exhibit obvious responses; a small increase (0.05 – 0.30 m) and no decreases were observed. The step changes in groundwater level in the west region (Chianan Plain), which is 30 km away from the epicenter, were relatively large and showed both increases and decreases (mostly increases). The distribution of the step changes in groundwater level is not consistent with the commonly used concept of epicentral distance, static stress–strain theory, or the focal mechanism. Moreover, the step changes in groundwater level showed both an increase and a decrease at different depths at a given location; these changes were due to different mechanisms.. Therefore, the mechanism of groundwater responses in sedimentary media is complex. An ideal static-stress model may not be suitable for such responses.

The dynamic stress effect can trigger changes in a groundwater system. The step increases in groundwater level at a shallow depth show a pattern that is consistent with the horizontal PGV, which implies that the increases in groundwater level may be induced by the pore water pressure buildup triggered by dynamic shear strain. However, other factors need to be considered to understand the complete mechanism. For the Meinong earthquake, the minimum horizontal PGV required to induce an obvious step change in groundwater level is 25 cm/s, and that required to induce soil liquefaction is 40 cm/s. Even though horizontal PGA did not show good agreement with step changes in groundwater level, we found that the approximate minimum horizontal PGA required to induce a step change in groundwater level is 120 cm/s^2 and that required to induce soil liquefaction is 160 cm/s^2. The ability to detect coseismic step changes in groundwater level with hourly sampling depends on the dissipation properties of the aquifer, which is determined by transmissivity and confinement. The wells that showed the responses were located in aquifers that had good confinement and small transmissivity. The minimum transmissivity required for groundwater level changes to persist long enough for hourly sampling is around 0.01 m^2/s. The integrated observations made during the Meinong earthquake indicate that ground motion and hydraulic properties are important factors in hydrological anomalies in sedimentary media. The results of this study provide an important reference for further studies on earthquake hydrology.

6. Data information

Hydrological data (hourly precipitation, river discharge, and groundwater level) of the Taiwan WRA were collected from the website https://gweb.wra.gov.tw/Hydroinfo/. Unfortunately, this website has no English version. The Taiwan WRA does not currently release raw data for public use. Users can only see time series graphs on the website. 1-Hz groundwater level data from the CWA can be found at the website https://gdms.cwa.gov.tw/. Registration is required to obtain the data. The GSMMA does not currently release raw 10-minute groundwater level data for public use. The monitoring well information can be found in Central Geological Survey (2015).

Author contributions

Shih-Jung Wang provided the research and illustration ideas, investigation suggestions and comments, supervised the analyses, and wrote and revised the manuscript. Yan-Yao Lin collected, arranged, and analyzed the data, prepared the tables, and drew the figures. Ying-Han Chen and Chia-Lin Chung reanalyzed some data and revised some figures. Wen-Chi Lai provided correction suggestions, technical support, and manuscript writing suggestions. Chien-Chung Ke provided comments and suggestions about the study results.

CRediT authorship contribution statement

Shih-Jung Wang: Writing – review & editing, Writing – original draft, Validation, Supervision, Resources, Project administration, Methodology, Funding acquisition, Data curation, Conceptualization, Formal analysis, Investigation, Software, Visualization. **Yan-Yao Lin:** Visualization, Validation, Software, Investigation, Formal analysis, Data curation. **Ying-Han Chen:** Visualization, Software, Investigation, Data curation. **Chia-Lin Chung:** Investigation, Formal analysis. **Wen-Chi Lai:** Validation, Software, Data curation. **Chien-Chung Ke:** Validation, Data curation.

Declaration of competing interest

The authors declare that they have no known competing financial interests or personal relationships that could have appeared to influence the work reported in this paper.

Acknowledgments

The authors would like to thank the Water Resources Agency, the Central Weather Administration, and the Geological Survey and Mining Management Agency of Taiwan for providing the hydrological monitoring data, geological survey data, and related information, the Earthquake-Disaster & Risk Evaluation and Management Center (E-DREaM) at National Central University for providing the earthquake information and PGA and PGV fields, and the Disaster Prevention Research Center, National Cheng Kung University, and the Graduate Institute of Applied Geology, National Central University, for providing the field survey data of soil liquefaction and surface rupture. The authors would also like to thank Professor Hone-Jay Chu at National Cheng Kung University and Dr. Wu-Cheng Chi at Academia Sinica, Taiwan, for providing valuable comments and suggestions to improve this study. This study was supported by the Ministry of Science and Technology (MOST), Taiwan, under grants MOST 109-2116-M-008-016, MOST 110-2116-M-008-003, and MOST 111-2116-M-008-007, and the National Science and Technology Council (NSTC), Taiwan, under grant NSTC 112-2116-M-008-004.

Appendix A. Supplementary data

Supplementary data to this article can be found online at https://doi.org/10.1016/j.jhydrol.2024.132230.

Data availability

The authors do not have permission to share data.

References

Akita, F., Matsumoto, N., 2004. Hydrological responses induced by the Tokachi-oki earthquake in 2003 at hot spring wells in Hokkaido. Japan. Geophysical Research Letters 31. https://doi.org/10.1029/2004GL020433.

Brodsky, E.E., Roeloffs, E., Woodcock, D., Gall, I., Manga, M., 2003. A mechanism for sustained groundwater pressure changes induced by distant earthquakes. J. Geophys. Res. 108 (8), 2390. https://doi.org/10.1029/2002JB002321.

Central Geological Survey, Taiwan, 2002. Research Report for Hydrogeological Survey in Pingtung Plain. (in Chinese).
Central Geological Survey, Taiwan, 2015. Observation of Groundwater Level and Investigation of Hydraulic Properties in Mountainous Areas in Southern Taiwan (2/4). (in Chinese).
Central Geological Survey, Taiwan, 2016. Geological Survey Report for 20160206 Earthquake. (in Chinese).
Chia, Y., Chiu, J.J., Jiang, Y.H., Lee, T.P., Wu, Y.M., Horng, M.J., 2008. Implications of coseismic groundwater level changes observed at multiple-well monitoring stations. Geophys. J. Int. 172, 293–301. https://doi.org/10.1111/j.1365-246X.2007.03628.x.
Cooper Jr, H.H., Bredehoeft, J.D., Papadopulos, I.S., Bennett, R.R., 1965. The response of well-aquifer systems to seismic waves. J. Geophys. Res. 70 (16), 3915–3926. https://doi.org/10.1029/JZ070i016p03915.
Cox, S.C., Rutter, H.K., Sims, A., Manga, M., Weir, J.J., Ezzy, T., White, P.A., Horton, T. W., Scott, D., 2012. Hydrological Effects of the Mw 7.1 Darfield (Canterbury) Earthquake, 4 September 2010, New Zealand. New Zealand Journal of Geology and Geophysics, https://doi.org/10.1080/00288306.2012.680474.
Dancey, C.P., Reidy, J., 2017. Statistics without maths for psychology: using SPSS for Windows, (8th ed.). Pearson.
Elkhoury, J.E., Brodsky, E.E., Agnew, D.C., 2006. Seismic waves increase permeability. Nature 441, 1135–1138. https://doi.org/10.1038/nature04798.
Feng, H., Liu, C.Y., Chuang, P.Y., & Chia, Y., 2016. Groundwater Level Changes Induced by the 2016 Meinong Earthquake. American Geophysical Union, Fall Meeting 2016, abstract #NH21A-1833.
Freeze, R.A., Cherry, J.A., 1979. Groundwater. Prentice-Hall.
Fu, C.-C., Walia, V., Yang, T.F., Lee, L.-C., Liu, T.-K., Chen, C.-H., Kumar, A., Lin, S.-J., Lai, T.-H., Wen, K.-L., 2017. Preseismic anomalies in soil-gas radon associated with 2016 M 6.6 Meinong earthquake, Southern Taiwan. Terr. Atmos. Ocean. Sci. 28, 787–798. https://doi.org/10.3319/TAO.2017.03.22.01.
Ge, S., Stover, C., 2000. Hydrodynamic response to strike- and dip-slip faulting in a half space. J. Geophys. Res. 105, 25513–25524. https://doi.org/10.1029/2000JB900233.
He, A., Singh, R.P., 2019. Groundwater level response to the Wenchuan earthquake of May 2008. Geomat. Nat. Haz. Risk 10 (1), 336–352. https://doi.org/10.1080/19475705.2018.1523236.
He, A., Fan, X., Zhao, G., Liu, Y., Singh, R.P., Hu, Y., 2017. Co-seismic response of water level in the Jingle well (China) associated with the Gorkha Nepal (Mw 7.8) earthquake. Tectonophysics 714, 82–89. https://doi.org/10.1016/j.tecto.2016.08.019.
He, A., Deng, W., Singh, R.P., Lyu, F., 2020. Characteristics of Hydroseismograms in Jingle Well. China. Journal of Hydrology 582, 124529. https://doi.org/10.1016/j.jhydrol.2019.124529.
Holzer, T.L., Youd, T.L., 2007. Liquefaction, ground oscillation, and soil deformation at the Wildlife Array, California. Bull. Seismol. Soc. Am. 97, 961–976. https://doi.org/10.1785/0120060156.
Hsu, Y.-F., Huang, H.-H., Huang, M.-H., Tsai, V.C., Chuang, R.Y., Feng, K.-F., Lin, S.-H., 2020. Evidence for fluid migration during the 2016 Meinong, Taiwan, aftershock sequence. J. Geophys. Res. Solid Earth 125, e2020JB019994. https://doi.org/10.1029/2020JB019994.
Huang, M.H., Hu, J.C., Ching, K.E., Rau, R.J., Hsieh, C.S., Pathierd, E., Fruneaue, B., Deffontainese, B., 2009. Active deformation of Tainan tableland of southwestern Taiwan based on geodetic measurements and SAR interferometry. Tectonophysics 466, 322–334. https://doi.org/10.1016/j.tecto.2007.11.020.
Huang, M.-H., Tung, H., Fielding, E.J., Huang, H.-H., Liang, C., Huang, C., Hu, J.-C., 2016. Multiple fault slip triggered above the 2016 Mw 6.4 MeiNong earthquake in Taiwan. Geophys. Res. Lett. 43, 7459–7467. https://doi.org/10.1002/2016GL069351.
Jonsson, S., Segall, P., Pedersen, R., Bjornsson, G., 2003. Postearthquake ground movements correlated to pore-pressure transients. Nature 424, 179–183. https://doi.org/10.1038/nature01776.
King, C.-Y., Azuma, S., Igarashi, G., Ohno, M., Saito, H., Wakita, H., 1999. Earthquake-related water-level changes at 16 closely clustered wells in Tono, central Japan. J. Geophys. Res. 104, 13073–13082. https://doi.org/10.1029/1999JB900080.
Kinoshita, C., Kano, Y., Ito, H., 2015. Shallow crustal permeability enhancement in central Japan due to the 2011 Tohoku earthquake. Geophys. Res. Lett. 42, 773–780. https://doi.org/10.1002/2014GL062792.
Kitagawa, Y., Itaba, S., Matsumoto, N., Koizumi, N., 2011. Frequency characteristics of the response of water pressure in a closed well to volumetric strain in the high-frequency domain. J. Geophys. Res. 116, B08301. https://doi.org/10.1029/2010JB007794.
Koizumi N., Lai, W.-C., Kitagawa, Y., & Matsumoto, Y., 2004. Comment on "Coseismic hydrological changes associated with dislocation of the September 21, 1999 Chichi earthquake, Taiwan" by Min Lee et al. Geophysical Research Letters, 31, L13603. https://doi.org/10.1029/2004GL019897.
Koizumi, N., Minote, S., Tanaka, T., Mori, A., Ajiki, T., Sato, T., Takahashi, H.A., Matsumoto, N., 2019. Hydrological changes after the 2016 Kumamoto earthquake. Japan. Earth Planets Space 71, 128. https://doi.org/10.1186/s40623-019-1110-y.
Kuo, T.-M.-C., Chen, W., Ho, C., 2018. Anomalous decrease in groundwater radon before 2016 Mw 6.4 Meinong earthquake and its application in Taiwan. Appl. Radiat. Isot. 136, 68–72. https://doi.org/10.1016/j.apradiso.2018.02.015.
Kuo, C.H., Wen, K.L., Hsieh, H.H., Lin, C.M., Chang, T.M., Kuo, K.W., 2012. Site Classification and Vs30 estimation of free-field TSMIP stations using the logging data of EGDT. Eng. Geol. 129–130, 68–75. https://doi.org/10.1016/j.enggeo.2012.01.013.
Lai, W.-C., Wang, S.-J., Hsu, K.-C., & Shieh, C.-L., 2016. The study of the coseismic groundwater level changes in Taiwan: An updated in ML 6.4 Tainan earthquake, Feb. 6th 2016. 15th Japan-Taiwan International Workshop on Hydrological and Geochemical Research for Earthquake Prediction. Tsukuba, Japan.
Lai, W.-C., Hsu, K.-C., Shieh, C.-L., Lee, Y.-P., Chung, K.-C., Koizumi, N., Matsumoto, N., 2010. Evaluation of the effects of ground shaking and static volumetric strain change on earthquake-related groundwater level changes in Taiwan. Earth Planets Space 62 (4), 391–400. https://doi.org/10.5047/eps.2009.12.008.
Le Beon, M., Huang, M.H., Suppe, J., Huang, S.T., Pathier, E., Huang, W.J., Chen, C.L., Fruneau, B., Baize, S., Hu, J.C., 2017. Shallow geological structures triggered during the Mw6.4 Meinong earthquake. Terr. Atmos. Ocean. Sci. 28 (5), 663–681. https://doi.org/10.3319/TAO.2017.03.20.02.
Lin, Y.Y., Yeh, T.Y., Ma, K.F., Song, T.R.A., Lee, S.J., Huang, B.S., Wu, Y.M., 2018. Source characteristics of the 2016 Meinong (ML 6.6), Taiwan, earthquake, revealed from dense seismic arrays: Double sources and pulse-like velocity ground motion. Bull. Seismol. Soc. Am. 108, 188–199. https://doi.org/10.1785/0120170169.
Liu, C.-Y., 2018. Temporal and Spatial Distribution of Hydrological Changes Induced by Earthquake, (Doctoral dissertation). National Taiwan University, Department of Geosciences in Chinese.
Lu, C.-C., Hwang, J.-H., Hsu, S.-Y., 2017. The impact evaluation of soil liquefaction on low-rise building in the Meinong earthquake. Earth Planets Space 69, 109. https://doi.org/10.1186/s40623-017-0693-4.
Lu, H.-Y., Liu, T.-K., Chen, W.-F., Peng, T.-R., Wang, C.-H., Tsai, M.-H., Liou, T.-S., 2008. Use of geochemical modeling to evaluate the hydraulic connection of aquifers: a case study from Chianan Plain. Taiwan. Hydrogeology Journal 16, 139–154. https://doi.org/10.1007/s10040-007-0209-6.
Lutzky, H.T., Lyakhovsky, V., Kurzon, I., Shalev, E., 2020. Hydrological response to the Sea of Galilee 2018 seismic swarm. J. Hydrol. 582. https://doi.org/10.1016/j.jhydrol.2019.124499.
M. Manga C.Y. Wang Earthquake hydrology Treatise on Geophysics 4 (2nd) 2015 Elsevier Oxford 305 328.
Manga, M., Rowland, J.C., 2009. Response of Alum Rock springs to the October 30, 2007 Alum Rock earthquake and implications for the origin of increased discharge after earthquakes. Geofluids 9 (3), 237–250. https://doi.org/10.1111/j.1468-8123.2009.00250.x.
Manga, M., Brodsky, E.E., Boone, M., 2003. Response of streamflow to multiple earthquakes. Geophys. Res. Lett. 30 (5), 1214. https://doi.org/10.1029/2002GL016618.
Manga, M., Beresnev, I., Brodsky, E.E., Elkhoury, J.E., Elsworth, D., Ingebritsen, S.E., Mays, D.C., Wang, C.Y., 2012. Changes in permeability caused by transient stresses: field observations, experiments, and mechanisms. Rev. Geophys. 50 (2), 1–24. https://doi.org/10.1029/2011RG000382.
Matsumoto, N., Kitagawa, G., Roeloffs, E.A., 2003. Hydrological response to earthquakes in the Haibara well, central Japan – I. Water level changes revealed using state space decomposition of atmospheric pressure, rainfall and tidal responses. Geophys. J. Int. 155, 885–898. https://doi.org/10.1111/j.1365-246X.2003.02103.x.
Midorikawa, S., Wakamatsu, K., 1988. Intensity of earthquake ground motion at liquefied sites. Soils Found. 28, 73–84. https://doi.org/10.3208/sandf1972.28.2_73.
Montgomery, D.R., Manga, M., 2003. Streamflow and water well responses to earthquakes. Science 300 (5628), 2047–2049. https://doi.org/10.1126/science.1082980.
Roeloffs, E.A., 1996. Poroelastic techniques in the study of earthquake-related hydrologic phenomena. in Advances in Geophysics, ed. R. Dmowska, Academic, San Diego, Calif. 137, 135–195. https://doi.org/10.1016/S0065-2687(08)60270-8.
Roeloffs, E.A., 1998. Persistent water level changes in a well near Parkfield, California, due to local and distant earthquakes. J. Geophys. Res. 103 (B1), 869–889. https://doi.org/10.1029/97JB02335.
Rojstaczer, S., Wolf, S., Michel, R., 1995. Permeability enhancement in the shallow crust as a cause of earthquake-induced hydrological changes. Nature 373, 237–239. https://doi.org/10.1038/373237a0.
Rutter, H.K., Cox, S.C., Dudley Ward, N.F., Weir, J.J., 2016. Aquifer permeability change caused by a near-field earthquake. Canterbury, New Zealand, Water Resources Research 52, 8861–8878. https://doi.org/10.1002/2015WR018524.
Seed, H.B., Idriss, I.M., 1982. Ground Motions and Soil Liquefaction during Earthquakes. Earthquake Engineering Research Institute Monograph, Oakland.
Sengupta, S., Sracek, O., Jean, J.-S., Lu, H.-Y., Wang, C.-H., Palcsu, L., Liu, C.-C., Jen, C.-H., Bhattacharya, P., 2014. Spatial variation of groundwater arsenic distribution in the Chianan Plain, SW Taiwan: Role of local hydrogeological factors and geothermal sources. J. Hydrol. 518 (C), 393–409. https://doi.org/10.1016/j.jhydrol.2014.03.067.
Shalev, E., Kurzon, I., Doan, M.-L., Lyakhovsky, V., 2016a. Sustained water Level changes caused by damage and compaction induced by teleseismic earthquakes. J. Geophys. Res. Solid Earth 121, 4943–4954. https://doi.org/10.1002/2016JB013068.
Shalev, E., Kurzon, I., Doan, M.-L., Lyakhovsky, V., 2016b. Water-level oscillations caused by volumetric and deviatoric dynamic strains. Geophys. J. Int. 204, 841–851. https://doi.org/10.1093/gji/ggv483.
Shalev, E., Lutzky, H., Kurzon, I., Lyakhovsky, V., 2021. Remote triggering of damage followed by healing recorded in groundwater pressure. Water 13, 3656. https://doi.org/10.3390/w13243656.
Shi, Z., Wang, G., Manga, M., Wang, C.Y., 2015. Continental-scale water-level response to a large earthquake. Geofluids 15, 310–320. https://doi.org/10.1111/gfl.12099.
Terzaghi, K., 1925. Erdbaumechanik auf boenphysikalischer grundlage. Deuticke, Vienna.
Ting, C.-S., Zhou, Y., de Vries, J.J., Simmers, I., 1998. Development of a preliminary ground water flow model for water resources management in the Pingtung Plain. Taiwan. Groundwater 35 (6), 20–36. https://doi.org/10.1111/j.1745-6584.1998.tb01062.x.

Tran, D.-H., Wang, S.-J., Chen, J.-Y., 2024. Mechanism of vertical displacement beneath shallow compression zone in coastal area. Earth Planets Space 76 (74). https://doi.org/10.1186/s40623-024-02019-2.

Wakita, H., 1975. Water wells as possible indicators of tectonic strain. Science 189, 553–555. https://doi.org/10.1126/science.189.4202.553.

Wang, S.-J., 2015. Dimensional upgrade approach for spatial-temporal fusion of trend series in subsidence evaluation. Entropy 17 (5), 3035–3052. https://doi.org/10.3390/e17053035.

C.-Y. Wang M. Manga Water and Earthquakes 2021 Springer Nature Switzerland.

Wang, C.-Y., Chia, Y., 2008. Mechanism of water level changes during earthquakes: near field versus intermediate field. Geophys. Res. Lett. 35, L12402. https://doi.org/10.1029/2008GL034227.

Wang, C.-Y., Cheng, L.H., Chin, C.V., Yu, S.B., 2001. Coseismic hydrologic response of an alluvial fan to the 1999 Chi-Chi earthquake. Taiwan. Geology 29, 831–834. https://doi.org/10.1130/0091-7613(2001)029<0831:CHROAA>2.0.CO;2.

Wang, S.-J., Lee, C.-H., and Hsu, K.-C., 2015a. A Technique for Quantifying Groundwater Pumping and Land Subsidence Using a Nonlinear Stochastic Poroelastic Model. Environmental Earth Sciences, 73(12), 8111-8124. https://doi: 10.1007/s12665-014-3970-6.

Wang, S.-J., Hsu, K.-C., Lai, W.-C., Wang, C.-L., 2015a. Estimating the extent of stress influence by using earthquake triggering groundwater level variations in Taiwan. J. Asian Earth Sci. 111, 373–383. https://doi.org/10.1016/j.jseaes.2015.06.030.

Wang, S.-J., Lee, C.-H., Chen, J.-W., Hsu, K.-C., 2015c. Combining gray system and poroelastic models to investigate subsidence problem in Tainan. Taiwan. Environmental Earth Sciences 73 (11), 7237–7253. https://doi.org/10.1007/s12665-014-3902-5.

Wang, S.-J., Hsu, K.-C., Wang, C.-L., Lai, W.-C., Hsu, L.-T., 2017. Evaluation of hydraulic properties of aquitards using earthquake-triggered groundwater variation. Groundwater 55 (5), 747–756. https://doi.org/10.1111/gwat.12519.

Wang, C.Y., Liao, X., Wang, C.H., Manga, M., 2016. Large earthquakes create vertical permeability by breaching aquitards. Water Resour. Res. 52, 5923–5937. https://doi.org/10.1002/2016WR018893.

Wang, C.-Y., Manga, M., 2010. Earthquakes and Water. Springer, New York.

Wang, C.-Y., Wong, A., Dreger, D.S., Manga, M., 2006. Liquefaction limit during earthquakes and underground explosions – implications on ground-motion attenuation. Bull. Seismol. Soc. Am. 96, 355–363. https://doi.org/10.1785/0120050019.

Wen, S., Yeh, Y.-L., Chang, Y.-Z., Chen, C.-H., 2017. The seismogenic process of the 2016 Meinong earthquake, southwest Taiwan. Terrestrial, Atmospheric Oceanic Sciences 28 (5), 651–662. https://doi.org/10.3319/TAO.2017.02.17.01.

Wong, A., Wang, C.-Y., 2007. Field relations between the spectral composition of ground motion and hydrological effects during the 1999 Chi-Chi (Taiwan) earthquake. J. Geophys. Res. Solid Earth 112, B10305. https://doi.org/10.1029/2006JB004516.

B.R. Wu M.W. Huang S.S. Ke W.S. Lee Mesh-Based Soil Liquefaction Analysis for Emergency Response-Case Study of the Meinong Earthquake in Taiwan 2017 Santiago, Chile.

Xue, L., Li, H.-B., Brodsky, E.E., Xu, Z.-Q., Kano, Y., Wang, H., Mori, J.J., Si, J.-L., Pei, J.-L., Zhang, W., Yang, G., Sun, Z.-M., Huang, Y., 2013. Continuous permeability measurements record healing inside the Wenchuan earthquake fault zone. Science 340, 1555–1559. https://doi.org/10.1126/science.1237237.

Yang, J., Sato, T., Savidis, S., Li, X.S., 2002. Horizontal and vertical components of earthquake ground motions at liquefiable sites. Soil Dyn. Earthq. Eng. 22 (3), 229–240. https://doi.org/10.1016/S0267-7261(02)00010-6.